Title: Disentangling the aging network of a termite queen

José Manuel Monroy Kuhn[1,2,*], Karen Meusemann[1,3] and Judith Korb[1,*]

[1] Department of Evolutionary Biology & Ecology, Institute of Biology I, Albert Ludwig University of Freiburg, Hauptstr. 1, D-79104 Freiburg (i. Brsg.), Germany

[2] Computational Discovery Research, Institute for Diabetes and Obesity, Helmholtz Zentrum München, Ingolstaedter Landstr. 1, D-85764 Neuherberg, Germany

[3] Australian National Insect Collection, CSIRO National Research Collections Australia, Clunies Ross Street, Acton, ACT 2601, Canberra, Australia

* corresponding authors: judith.korb@biologie.uni-freiburg.de; manuel.kuhn@helmholtz-muenchen.de

Abstract

Background: Most insects are relatively short-lived, with a maximum lifespan of a few weeks, like the aging model organism, the fruit-fly *Drosophila melanogaster*. By contrast, the queens of social insects (termites, ants, some bees and wasps) can live for more than a decade. This makes social insects promising new models in aging research providing insights into how a long reproductive life can be achieved. Yet, aging studies on social insect reproductives are hampered by a lack of quantitative data on age-dependent survival and time series analyses that cover the whole lifespan of such long-lived individuals. We studied aging in queens of the drywood termite *Cryptotermes secundus* by determining survival probabilities over more than 15 years and performed transcriptome analyses for queens of known age that covered their whole lifespan.

Results: The maximum lifespan of *C. secundus* queens was 13 years with a median maximum longevity of 11.0 years. Time course and co-expression network analyses of gene expression patterns over time indicated a non-gradual aging pattern. It was characterized by networks of genes that became differentially expressed only late in life, namely after an age of 10 years, which associates well with the median maximum lifespan for queens. These old-age gene networks reflect processes of physiological upheaval. We detected strong signs of stress, decline, defence and repair at the transcriptional level of epigenetic control as well as at the post-transcriptional level with changes in transposable element activity and the proteostasis network. The latter depicts an upregulation of protein degradation, together with protein synthesis and protein folding, processes which are often down-regulated in old animals. The simultaneous upregulation of protein synthesis and autophagy is indicative for a stress-response mediated by the transcription factor *cnc*, a homolog of human *nrf* genes.

Conclusion: Our results show non-linear senescence with a rather sudden physiological upheaval at old-age. Most importantly, they point to a re-wiring in the proteostatis network as central for explaining the long life of social insect queens.

Keywords

RNASeq, transcriptomes, ageing, social insects, weighted gene co-expression networks, WGCNA, time series, termite, lifespan, senescence

Background

Almost all animals age, but at different pace [1]. The fruit fly *Drosophila melanogaster* lives only for around seven weeks [2], while the clam Ocean Quahog, *Arctica islandica*, can have a lifespan of more than 400 years [3]. Generally, organisms with large differences in rates of aging are found between widely divergent species [1,4], which makes controlled comparisons of the underlying aging mechanisms difficult.

Classical model organisms typically have a short lifespan and can be characterized by r-life history strategies ('live fast, have many offspring and die young') as exactly these traits make them good model organisms. Social insects such as termites, ants, or the honeybee, offer promising new insights into aging research because individuals with the same genetic background can differ by orders of magnitudes in lifespan. Within a social insect colony, which is generally a large family, the reproducing queen (and in termites, also the king) can reach lifespans of more than 20 years, while non-reproducing workers have a lifespan of a few months only [5-8]. However, quantitative demographic data covering the whole lifespan of queens are inherently rare and many reports on queen-longevity are more anecdotal. Thus, it is largely unknown for long-lived queens whether they age gradually or whether aging is a more sudden event.

During recent years, several pioneering studies, especially on the honeybee, revealed exciting new insights into the mechanisms of how queens can live so long. In the honeybee, juvenile hormone (JH) seems to have lost its direct gonadotropic function in adults so that queens have a high expression of the yolk precursor gene vitellogenin (*Vg*) without requiring high JH titres (*e.g.*, [9,10]). This result has led to the hypothesis that uncoupling JH and *Vg* expression might account for the long life of honeybee queens [9] as well as social insect queens more generally [11] because the life-time shortening consequences of high JH titers are absent. However, this re-wiring along the JH-*Vg* axis is not universal for all social Hymenoptera, since the queens of many other ant and bee

species require JH for vitellogenesis (*e.g.* [12] and references therein). For termites, fewer studies exist, but JH is required for vitellogenesis [13,14]. Hence, other mechanisms must exist to explain the long life of termite queens. Studies of the subterranean termite *Reticulitermes speratus* implicated the involvement of a *breast cancer type 1 susceptibility (BRCA1*) homolog [15], which is involved in DNA repair [16], and better protection against oxidative stress by superoxide dismutases and catalases [17,18]. The latter have also been discussed for other social Hymenoptera, including ants and the honeybee. Yet overall evidence of the role of oxidative stress is less clear (reviewed in [19-21]). Furthermore, regulation of the activity of transposable elements (TEs) [22], and changes in the insulin/insulin-like growth factor1 signalling (IIS) and target of rapamycin (TOR) pathways [23] have been linked with caste-specific aging differences in termites. Both, the TOR and IIS pathway, have been associated with longevity in model organisms from *D. melanogaster* to mice and humans [24-26]. They are the most intensively studied aging related pathways and they have also been associated with caste differences in social Hymenoptera (*e.g.*, [27-31]). Yet, all studies on social insects suffer from a lack of time-series data to investigate molecular changes across the lifespan of long-lived queens. Like the demographic life history data, such data are inherently difficult to obtain due to the long lifespan of queens. However, they are necessary (i) to understand the aging process, (ii) to work out potential changes compared to solitary insects, and (iii) to identify the relevant age-classes for detailed studies. The latter is a completely overlooked issue but highly relevant. If, for example, aging is a non-linear process, differences across studies might just be consequences of none-comparable age-classes between studies.

We studied aging in termite queens of known age across their entire lifespan to measure at the ultimate, eco-evolutionary level age-dependent survival and at the proximate, mechanistic level age-specific changes in gene expression. For the latter, we generated head and thorax

transcriptomes of queens of different age (for an outline of the workflow see Additional File 1, Figure S1). We used field collected, newly established colonies of the wood-dwelling termite *Cryptotermes secundus* (Hill, 1925) (Blattodea, Isoptera, Kalotermitidae) that were kept under identical conditions in the laboratory for a time span of 15 years. Keeping them under constant and optimal conditions allowed us to study intrinsic aging, disentangled from causes of extrinsic mortality such as predation, food shortage, or disease. As typical for wood-dwelling termite species, *C. secundus* colonies are founded in a piece of wood, which serves as food and shelter and which workers never leave to forage outside. Such species have a low social complexity with small colonies and totipotent workers that develop into sexuals.

Results

Survival analysis

Overall, we had surviving founding queens from an age of two years up to a maximum of 13 years. The potentially 14- and 15-year old queens all had died as had most queens with a potential age of ≥ 12 years. Out of eight queens in this 'old-age' class, only a single queen (13 years) had survived (Fig. 1). The median longevity of the queens in the laboratory after successful colony establishment was estimated with Kaplan Meier survival analysis to be 12.0 years (SE: ± 0.54) (mean longevity: 11.1 years, SE: ± 0.66) (Fig. 1).

Identifying transcripts that change their expression with age: age-related DETs

To study gene expression changes over the lifetime of queens we generated transcriptomes of head and thorax from twelve queens with different chronological age since onset of reproduction, from two until 13 years, covering the complete lifespan of *C. secundus* queens: 2, 3, 4, 5, 6, 7, 8, 9, 10 (two samples), 11, and 13 years (Additional File 2, Table S1).

A total of 169 transcripts were significantly differentially expressed (DETs) over time as revealed by Iso-MaSigPro time series analysis (Additional File 2, Table S2). According to their expression pattern, DETs were grouped into six Iso-MaSigPro clusters (hereafter, 'cluster') (Fig. 2). Cluster 1 represented 44 DETs, which were slightly expressed in young queens followed by a decline at middle ages and a strong increase when queens became older. The 32 DETs of cluster 2 characterized young queens with a declining expression with age. Clusters 3 and 5 comprised 31 and 37 DETs, respectively, that were highly expressed in middle aged queens, while cluster 4 and cluster 6 (15 and 10 DETs) characterized old queens with no expression in young ones. Thus, in the following we referred to the DETs as young (cluster two), middle-aged (clusters three and five) and old DETs (clusters one, four and six). Details for all clusters are provided in Additional File 2, Table S2.

Identifying modules of co-expressed transcripts

To identify modules of co-expressed transcripts, we performed a weighted gene co-expression network analysis (WGCNA). It revealed a total of 254 modules of co-expressed transcripts. Based on eigengene values, 13 modules correlated significantly positively with age and 13 negatively (see Additional File 1, Figures S2 and S3; Additional File 3 (WGCNA module-age association, shown are eigengene values for all modules).

Identifying transcript co-expression modules with age-related DETs

Within the age-correlated WGCNA modules, we identified age-related DETs. The negatively age-correlated module 'seashell4' had the highest number of young DETs (10 DETs). No gene ontology (GO) term was enriched for this module. The highest number of old DETs were found in the positively age-correlated modules 'cyan' (89 DETs) and 'tan' (79 DETs) (Additional File 2, Table

S3 and S4). Only broad categories were enriched in the 'cyan' module (*e.g.* RNA metabolic process and gene expression) and the 'tan' module was enriched for ribosomal and tRNA related functions (Additional File 1, Figure S4).

Extracting age-related subnetworks based on age-related DETs

To generate subnetworks related to the age-related DETs, we located them in the WGCNA co-expression network. These DETs and their one- and two-step neighbors (*i.e.*, the 'second level neighborhood') were then extracted from the co-expression network, which resulted in 50 subnetworks of different sizes (for more details see Methods) (Additional File 1, Figure S5). Note, DETs might be located at the boundaries of multiple WGCNA modules which means the subnetworks obtained consist of fragments of multiple WGCNA modules. The resulting subnetworks either contained young and middle-aged DETs or old DETs, with a single exception where a middle-aged DET was in the periphery of the largest subnetwork containing old DETs. The largest subnetwork containing either young and middle-aged DETs (hereafter, young subnetwork) or old DETs (plus a single middle-age DET; hereafter old subnetwork) were further analyzed.

Young subnetwork

The largest young subnetwork comprised 164 transcripts (out of these 24 Iso-MaSigPro DETs) of which only 12 (7%) were one-to-one orthologs to *D. melanogaster* genes (Additional File 2, Table S3). The GO enrichment analysis of the young subnetwork showed multiple Biological Process (BP) terms related to RNA catabolism, but these GO terms were not significant after correcting for multiple testing (Additional File 2, Figure S6).

TE activity and genome instability. 53 DETs (32%) of the young subnetwork were related to TEs (Fig. 3 and Additional File 2, Table S3), comprising TEs and genes from TE defense pathways. This included one homolog of the gene *argonaute 2* (*ago2*) (two transcripts), an essential gene of the endo-siRNA pathway which silences TEs [32], and *arsenite 2* (*ars-2*) which is required for siRNA and miRNA-mediated TE silencing [33]. Additionally, we found two genes connected to DNA damage response and genome instability: *kin17* and *PIF1-like* gene.

Other signatures. From well-known aging pathways, we identified (i) *inositol polyphosphate phosphatase 2* (*mipp2*) and (ii) *adenylyl cyclase 76E* (*ac76E*). The former is part of the TOR pathway and has been associated with longevity [34] and the latter is activated by the transcription factor 'Forkhead box O' (*foxo).* Additionally, we found several fecundity related DETs. They included two transcripts of the gene *hu li tai shao* (*hts*) (one a DET of IsoMaSigPro cluster two) and one homolog of the gene *bällchen* (*ball*) (two transcripts) (one a DET of cluster five, Fig. 3)

Old subnetwork

The largest 'old subnetwork' comprised 1,098 transcripts (out of these 42 Iso-MaSigPro DETs). 521 transcripts (47%) were identified as one-to-one orthologs of *D. melanogaster* genes (Additional File 2, Table S4). Iso-MaSigPro DETs in the old subnetwork belonged mainly to Iso-MaSigPro clusters 1 and 4. The second level neighborhoods of these DETs were connected in the network and a GO enrichment analysis revealed multiple GO terms associated with protein related functions, including translation, protein folding, unfolded protein binding, proteolysis involved in cellular protein catabolic process, protein targeting to ER, ribosome, and proteasome complex (Additional File 1, Figures S7 and S8). 198 transcripts of the old subnetwork (18%) were involved in protein translation, protein folding, and protein catabolism and proteolysis (Figs. 4 and 5 [35,36] and

Additional File 2, Table S4). Additionally, 61 transcripts (~6%) were related to TEs (Additional File 2, Table S4).

Epigenetic modifications, transcriptional regulation, and TE activity. Many genes of the old subnetwork are involved in de/acetylation and methylation of DNA, which are important epigenetic modifications that regulate gene expression and genome stability [37-39] (Additional File 2, Table S4).

Most strikingly, two crucial histone acetylation modifying complexes, the Tip60 acetyltransferase complex and the male specific lethal (msl) complex were represented in the old subnetwork. The former included the genes *dom, ing3, mrg15, pont* and *rept*, and the latter *msl-1, msl-3* and *mof*. Genes involved in deacetylation of DNA were, for instance, *sirtuin 1* (*sirt1*), *histone deacetylase 3* (*HDAC3*), and *histone deacetylase 6* (*HDAC6*). Genes linked to epigenetic histone methylation included, for instance, *ash-1* and *lid*. Another well represented group of genes connected to expression regulation in the old subnetwork were spliceosome components and splicing factors. Additionally, we found in the old subnetwork important transcripts related to TE silencing: *dicer-2, Hsc70-4, Hsc70-3, Hsp83, trsn, armi, Rm62, Gasz, Tudor-SN*, and *Hel25E*. Details are given in Additional File 2, Table S4.

Proteostasis and oxidative stress. Related to proteostasis we detected a strong signal for protein synthesis and degradation. Regarding protein synthesis, the old subnetwork comprised many transcripts coding for initiation, elongation and termination factors, as well as many ribosomal proteins and aminoacyl-tRNA synthetases (Fig. 4; Additional File 2, Table S4). Regarding protein degradation, almost all subunits of the ubiquitin proteasome system (UPS) were present (Fig. 5) as well as autophagy genes, heat shock proteins, and the transcription factor *xbp1*. *Xbp1* is involved in

the 'unfolded protein response' (UPR) and in the ER-associated protein degradation (ERAD) pathway [40,41].

Additionally, *BRCA1* was also present in the old subnetwork. This gene is involved in oxidative stress response, and in the transcriptional activation of proteasomal genes by stabilizing the transcription factor *cnc*/*nrf-2* (*cap-n-collar/nuclear factor erythroid 2–related factor 2*) [42]. Other genes in the old subnetwork involved in oxidative stress response and transcriptionally activated by *nrf-2* were thioredoxin and S-glutathione transferase.

Other signatures. Additionally, the old subnetwork was characterized by a signature of ecdysone biosynthesis with *ecdysone receptor* (*EcR*), *ecdysone-induced protein 75B* (*Eip75B*), *phantom* and *disembodied*. The presence of *Phosphotidylinositol 3 kinase 68D (Pi3K92E)* links to the IIS pathway.

Locating age-related co-expression modules in the age-related subnetworks

Finally, we inspected those WGCNA modules with a large fraction of transcripts in the young and old subnetworks as well as those modules that were significantly associated with age.

In the young subnetwork, WGCNA modules with a large fraction of transcripts were 'saddlebrown' and 'skyblue4' which both did not significantly correlate with age. Significantly age-correlated co-expression modules were firebrick2, indianred1 and seashell4 (Additional File 1, Figure S2). No GO terms were significantly enriched for any of these modules.

In the old subnetwork, the modules with a large fraction of transcripts were 'green' and 'paleturquoise' which again did no significantly correlate with age. The old subnetwork contained transcripts of 13 significantly age-correlated co-expression modules (Additional File 1, Figure S3).

234 The GO enrichment analysis of these modules revealed several terms involved in protein related
235 functions, including ribosome biogenesis, rRNA processing, protein folding, translation, unfolded
236 protein binding, protein catabolic process, protein transport, tRNA aminoacylation for protein
237 translation, and proteasome core complex (Additional File 1, Figure S4, S9, S10 and Additional
238 File 4, Table S5).
239

240 ## Discussion

241 Our study revealed a median maximum reproductive longevity of *C. secundus* queens of 12 years
242 with a maximum lifespan of 13 years when excluding all causes of extrinsic mortality in the
243 laboratory. The curve suggests a rather sudden decline in live expectancy after an age of around 11
244 years; out of eight queens with a potential age ≥ 12 years, all had died, except one 13-year old
245 queen (Fig. 1). The survival curve indicates a type I survivorship, after queens have successfully
246 founded a colony and without extrinsic mortality.
247

248 Our transcriptome study identified six clusters of transcripts that were significantly differentially
249 expressed with age (DETs) (Fig. 2): one cluster for young queens (cluster 2), two for medium aged
250 queens (cluster 3 and 5) and three for old queens (cluster 1, 4, and 6). This implies that three
251 'molecular' life stages can be distinguished in *C. secundus* queens with the third corresponding to
252 old, aged queens that will probably die soon as no queen reached a lifespan beyond 13 years. The
253 co-expression network analysis, which extracted subnetworks based on age-related DETs, resulted
254 in two main subnetworks, a young and an old subnetwork. This implies that there are two *age-*
255 *related* 'molecular' life stages, as DETs/genes of young and medium ages belonged to the same
256 young subnetwork.
257

Young subnetwork

The young subnetwork contained DETs characteristic for young and medium ages. This shows the similarity in expression of these two age stages. Not unexpectedly, the young subnetwork indicates an upregulation of transcripts linked with fecundity (*e.g., hts*, *ball*) and of the TOR pathway (*mipp2*) which has been associated with longevity [34]. The upregulation of *Ac76E* may imply that the IIS pathway is down because this gene is activated by the transcription factor foxo which is inhibited by an upregulated IIS pathway. However, other evidence suggests that, like in other social insects (*e.g.* [12] and references therein), queens are characterized by an upregulated IIS pathway [23]. Additionally, we detected several upregulated TEs-related transcripts associated with signs of an upregulation of the endo-siRNA pathway (*e.g. ago2*, *ars*) which is a transcriptional and post-transcriptional TE-defence mechanism of the soma [32,33,43] (Kim, Lee and Carthew, 2007; Sabin *et al.*, 2009; Piatek and Werner, 2014).

Old subnetwork

The old subnetwork contained many more transcripts (1,098 vs. 164 in the young subnetwork). Our results imply a physiological stage of upheaval shortly before queens die. There were strong signs of decline and repair at the upstream transcriptional level of epigenetic control as well as at the posttranscriptional level of TE-activity and the proteostasis network.

Epigenetic modifications

An upregulation of genes modifying histone marks implied considerable epigenetic changes that lead to altered gene expression as is typical for aging organisms:

First, our results indicate dynamic changes of ‘active’ histone marks of euchromatin because many genes related to H3K4 and H3K36 de/methylation and H4K16 de/acetylation were present in the

old subnetwork (Additional File 2, Table S4). For instance, the Tip60- as well as the msl-complex were well represented. Both complexes are involved in acetylation of histones, including H4K16, which, for instance, is indicative for replicative aging in yeast [44]. The upregulation of *Sirt1* may function as an antagonist as it deacetylates H4K16. The same applies for the deacetylases HDAC6 and HDAC3, which can also deacetylase histones [39].

Second, there is also evidence for changes of repressive histone mark of heterochromatin (*e.g.* linked to H3K9 and H3K27 acetylation) (Additional File 2, Table S4). For instance, the old age transcript ALP1 is an antagonist of HP1, the latter is involved in the maintenance of heterochromatin. HP1 generally decreases with age, and its overexpression can lead to an increased lifespan in *D. melanogaster* [45,46].

TE activity

In line with a deregulation of repressive histone mark of heterochromatin, several TE-related transcripts were also connected with the old subnetwork (Additional File 2, Table S4). TEs often are accumulated in heterochromatin which silences their activity [47]. Yet, dysregulation of heterochromatin can allow them to become active and this has been associated with aging [48,49]. Also the upregulation of several genes from two TE-defense pathways - the endo-siRNA pathway (*e.g. dicer2*, *Hsc-70-4*, *trsn*) as well as the of piRNA pathways (*e.g.*, piRNA biosynthesis. *armi*, *gasz*, *Hel25E*, *Rm62*; ping-pong cycle: *Tudor-SN*, *qin*) - support the notion of active TEs. Both pathways silence TEs posttranscriptionally [50-52]. TE activity and especially the piRNA pathway has also been associated with aging and the longevity of termite reproductives in another termite species [22].

Loss of proteostasis

Our results revealed a very strong proteostasis signal indicative for an upheaval in protein synthesis, protein folding and protein degradation in old queens. Many genes from the proteostasis network were detected in the old subnetwork (Additional File 2, Table S4). They indicate an upregulation of protein degradation, together with protein synthesis and protein folding (Figs. 4 and 5). This is unusual because old organisms are typically characterized by a downregulation of all these processes (Fig. 6).

Protein synthesis. Many transcripts coding for ribosomal proteins and aminoacyl-tRNA synthetases were found in the old subnetwork, indicative of upregulated protein synthesis (Additional File 2, Table S4). This is further supported by a strong signal of an active TORC1 system which promotes protein synthesis (Fig. 7 [53-55]). Thus, for instance, many downstream eukaryotic initiation factors (eIF4A, eIF4B, eIF4E, eIF4G) and eukaryotic elongation factor (eEF2) transcripts were found in the old subnetwork (Fig. 4). They activate, ribosome biogenesis, translational elongation, and cap-dependent translocation (Fig. 7).

Protein degradation. Normally, an active TORC1 system is associated with a downregulation of protein degradation as it inhibits proteolytic systems [54-56] and autophagy (*e.g.*, upregulated TORC1 inhibits ATG1, which is necessary for autophagy activation; Fig. 7). Surprisingly, however, we found strong evidence of upregulated protein degradation in the old subnetwork. Several transcripts linked to autophagy, almost all subunits of the UPS, the UPR-, and the ERAD pathway as well as heat shock proteins characterized the old subnetwork (Figs. 5 and 6; Additional File 2, Table S4).

329 *Linking protein synthesis and degradation.* The simultaneous upregulation of protein synthesis and
330 autophagy might be explained by a stress response. In *D. melanogaster* as well as in humans, under
331 stress conditions upregulated TORC1 enhances an oxidative stress response, controlled by the
332 transcription factor *cnc*, a homolog of human *nrf* genes (Fig. 7). Ubiquitinated proteins and
333 damaged mitochondria activate *cnc/ nrf-2* via p62, supported by upregulated TORC1, which then
334 activates oxidative stress response genes [57,58] (Ichimura *et al.*, 2013; Aramburu *et al.*, 2014).
335 Additionally, *cnc* is known to activate chaperones (protein folding) and the proteasome [59], and
336 this has been associated with lifespan expansion in *D. melanogaster* and *Caenorhabdtis elegans*
337 [60,61].
338 Support for the conclusion of a stress-associated, active *cnc* transcription factor in old queens
339 comes from several transcripts in the old subnetwork (Fig. 7): (i) BRCA1, which indirectly actives
340 *cnc* by inhibiting *cnc* inhibitor *Keap1*, and (ii) the *Tip 60* complex as well as genes that are
341 transcriptionally activated by *cnc*, such as *thioredoxin, S-Glutathione transferases* and *UPS* genes
342 (Fig. 7).
343 Hence, our results imply that old *C. secundus* queens are in a stage of stress. They have mounted
344 stress response systems mediated by *cnc*, including protein degradation and protein folding.
345 However, it is unusual that old queens can do this. In *D. melanogaster*, only young individuals can
346 mount this stress response [59] (Tsakiri *et al.*, 2013). The constant activation of the proteasome in
347 these very old queens may lead to their death (note, the studied queens had reached their maximum
348 lifespan, we never had older queens) as the constant activation of the proteasome in transgenic flies
349 was detrimental for survival [59].
350
351 **Comparison with other social insects**

There has been a debate about the role of oxidative stress to explain the long lifespan of social Hymenoptera queens; yet evidence is inconclusive (*e.g.* reviewed by [19-21]). For instance, markers of oxidative stress in the brain of honey bee workers do not increase with age, although they live shorter than queens [62]. In the ant *Lasius niger*, both workers and males show higher activity of the antioxidant superoxide dismutase than queens, but both live shorter than queens [63]. These studies have shown that higher expression of oxidative stress response genes do not necessarily correlate with longer lifespans. For the termite *Reticulitermes speratus*, it has been suggested that queens are better protected against oxidative stress as qRT-PCRs studies showed a higher expression of the antioxidants catalases and peroxiredoxins in queens compared to workers [17], while kings were characterized by a high expression of *BRCA1* (in the fat body) compared to workers [15]. Unfortunately, the age of the studied reproductives is not known. It would be of interest to study expression of these genes with age, as this would contribute to a better understanding of the aging process but such studies are rare.

Conclusion

Our results imply that *C. secundus* queens do not age gradually, rather at old age there is a physiological stage of upheaval, characterized by signs of stress (activity of TEs, active *crc*) and defense (piRNA pathways) / repair (protein degradation and synthesis) before the animals die. This apparently sudden decline is in line with the few life history records of social insect queens that exist. They also found no signs of gradual senescence but an abrupt death (*e.g.*, the ant *Cardiocondyla obscurior* [64]; see also Fig. 1). This stresses the importance of using queens of known age for aging studies as processes revealed from middle-aged versus old queens probably

376 differ considerably. Our study is the first addressing the aging process for a social insect by

377 studying the complete lifespan of queens.

Methods

Figure S1 (Additional File 1) provides a schematized workflow of the analyses described in the following sections.

Collection and colony maintenance

From 2002 until 2016, *C. secundus* colonies were collected from mangroves near Palmerston - Channel Island (12°30' S, 131°00' E; Northern Territory, Australia) when they were less than one year old [65]. Colonies of an age of less than one year can be identified by the size and slightly lighter sclerotization of the founding reproductives (primary reproductives), the presence of less than 20 workers and short tunnel systems of a few centimeters. All collected colonies were transferred to *Pinus radiata* wood blocks and transported to the laboratory in Germany, where they were kept under standardized conditions in a climate room with a temperature of 28 °C, 70% humidity and a 12h day/night rhythm (Additional File 2, Table S1). Under these conditions, colonies develop like in the field (see [66]). Up until 2019 wood blocks were split and the colonies were extracted to determine survival of reproductives.

Survival analysis

The survival of primary queens (and kings) was determined by their presence /absence. Founding (primary) queens can be identified by their dark brown color, compound eyes and wing abscission scars. If the primary reproductives had died and the colony was still alive, they had been replaced by neotenic replacement reproductives which lack these traits. The median longevity of queens was determined using Kaplan Meier survival analysis in SPSS 23 [67]. Only colonies that survived the transfer from the field to the laboratory in Germany and the re-establishment in the new wood block were used for this analysis. This resulted in a sample size of 41 colonies. Overall, we had surviving

primary queens from an age of one year up to a maximum of 13 years. The three potentially 14- and 15-year old queens were all dead.

Transcriptome study

RNA extraction and sequencing

RNA was extracted from twelve queens with different chronological age since onset of reproduction from two years until 13 years: 2, 3, 4, 5, 6, 7, 8, 9, 10 (two samples), 11, and 13 years. In colonies older than 13 years, the original queen was always replaced by a neotenic replacement queen.

An in-house protocol was followed for RNA extraction (see [23]). Individuals were placed on ice and the gut was removed and discarded. The head together with the thorax were used for RNA extraction. Samples were transferred into peqGOLD Tri Fast™ (PEQLAB) and homogenized in a Tissue Lyser II (QIAGEN). Chloroform was used for protein precipitation. From the aqueous phase, RNA was precipitated using Ambion isopropyl alcohol and then washed with 75% ethanol. Obtained pellets were solved in nuclease-free water. DNA was subsequently digested using the DNase I Amplification Grade kit (Sigma Aldrich, Cat. No. AMPD1). We performed an RNA Integrity Number Analysis (RIN Analysis) measuring the RNA concentration with the Agilent RNA 6000 Nano Kit using an Agilent 2100 Bioanalyzer (Agilent Technologies) for quality control. Samples with total RNA were sent on dry ice to Beijing Genomics Institute (BGI) Tech Solutions (HONGKONG) Co. and then to the BGI-Shenzhen (PR China) for sequencing. The preparation of the cDNA libraries was performed by BGI according to their internal and proprietary standard operating procedure. The cDNA libraries were paired-end sequenced (not-strand specific) on Illumina HiSeq 2500 and 4000 platforms (100 base pairs read length and about 4 Giga bases per sample). Index sequences from the machine reads were demultiplexed and a quality -check and

filtering of raw reads was done using the package soapuke (-n 0.05 -l 20 -q 0.2 -p 1 -i -Q 2 -G --seqType 1 and -A 0.5, http://soap.genomics.org.cn/).

Processing of RNASeq raw reads

FastQC (v0.11.4) [68] was used to evaluate the quality of the cleaned raw reads. To obtain a transcript count table, the cleaned raw reads were pseudo-aligned with Kallisto (default settings, v0.43.0) [69] (Bray *et al.*, 2016) against a *C. secundus* transcriptome obtained from a draft version of the *C. secundus* genome (with estimated gene and transcript models, see [23,70]. The counts estimated by Kallisto were normalized using DESeq2 (v1.18.1, count/size factor) [71] in R (v3.4.4) [72].

Time course analysis to identify age-associated differentially expressed transcripts (DETs)

The normalized counts were used as input for the R package Iso-MaSigPro (v1.50.0) [73] to test for differentially expressed transcripts (DETs) across time. Iso-MaSigPro is designed for the analysis of multiple time course transcriptome data. It implements negative binomial generalized linear models (GLMs) [73,74]. Significantly differentially expressed transcripts (FDR corrected p-value set to 0.05) were clustered using the clustering algorithm mclust in Iso-MaSigPro [73] resulting into six Iso-MaSigPro clusters (Additional File 2, Table S2).

Weighted Gene Co-expression Network Analysis (WGCNA) to identify networks of co-expressed transcripts

To obtain networks of co-expressed transcripts that were categorized as modules we performed a Weighted Gene Co-expression Network Analysis (WGCNA). The counts obtained with Kallisto (v0.43.0) [69] were transformed using variance stabilizing transformation (vst) as implemented in

DESeq2 (v1.18.1) [71]. The vst transformed counts were used to perform a co-expression network analysis with the R package WGCNA (v1.63) [75]. For more details on the methodology, see [75-77]. In short, (Additional File 1, Figure S1, workflow, right side), a similarity matrix was built by calculating Pearson correlations between the expression values of all pairs of transcripts. Using the similarity matrix, a signed weighted adjacency matrix was obtained as described by the formula:

$$a_{ij} = \left(\frac{1}{2}\left(1+\mathrm{cor}_{ij}\right)\right)^{\beta}$$

Where cor_{ij} is the Pearson correlation between the expression pattern of transcript 'i' and transcript 'j' (the similarity value). The value of β was chosen based on the soft-thresholding approach [75]. With this value of β, we obtained a weighted network with an approximate scale-free topology (β=14, scale-free topology $R^2 = 0.84$). In a signed weighted adjacency matrix negative and small positive correlations get negligibly small adjacency values shifting the focus on strong positive correlations. Seeing the adjacency matrix as a network, the nodes correspond to the transcripts and the connections between nodes correspond to the adjacency values (transformed correlation coefficients). A topological overlap matrix (TOM), which in addition to the adjacency matrix considers topological similarity (shared neighbors reinforce the connection strength between two nodes), was constructed using the adjacency matrix [78]. To define transcript modules, a hierarchical clustering tree was constructed using the dissimilarity measure (1-TOM). Transcript modules were defined by cutting the branches of the tree using the Dynamic Hybrid Tree Cut algorithm [79] and the minimum module size was set to 30 transcripts. Transcript modules with similar expression profile were merged by hierarchical clustering of the eigengene correlation values. Briefly, a hierarchical clustering tree was created with the eigengene dissimilarity measure (1-correlation coefficient of eigengenes) and a tree height cut of 0.20 was used (corresponds to a eigengene cor ≥ 0.80). Eigengenes were calculated with the function moduleEigengenes (default settings) [75]. A module eigengene corresponds to the first principal component of the module and

can be seen as a weighted average expression profile [75]. To find significantly associated modules with age, correlations between age and eigengenes of the merged modules were calculated. Each module was named after a color by WGCNA.

The adjacency matrix of the WGCNA was visualized using Cytoscape (v3.7.1) [80], only including pairs of nodes with a $cor_{ij} \geq 0.90$. The color of each module corresponds with the respective module name (*e.g.*, saddlebrown color for the saddlebrown module).

To identify co-expression modules containing age-related DETs, we looked for age-related DETs from the Iso-MaSigPro analysis in the WGCNA modules. Those modules which were significantly correlated with age and which contained the highest number of Iso-MaSigPro DETs were further inspected.

Identifying/Extracting age-related subnetworks based on age-related DETs

To identify age-related subnetworks within the co-expression network, we combined the results of the Iso-MaSigPro analysis with those from the WGCNA and extracted subnetworks that were based on age-related Iso-MaSigPro DETs. Therefore, we extracted 1st and 2nd neighbors of DETs based on the WGCNA co-expression network (*i.e.*, the visual representation of the adjacency matrix). To do this, we used the 'First neighbors' function of Cytoscape. We selected an age-related DET from Iso-MaSigPro as transcript of interest. By calling the function, the neighboring transcripts were selected, which were then extracted to form a subnetwork. By calling the function twice, one obtains the one- and two-step neighbors (called 'second level neighborhood') of the transcript of interest. This was done for each DET identified in IsoMaSigPro.

The obtained subnetworks were clearly separated in those containing young Iso-MaSigPro DETs (young subnetworks) and those containing old Iso-MaSigPro DETs (old subnetworks). The largest subnetwork obtained for each group was used for further analysis paying attention to both, transcript identity as well as WGCNA module content. Thus, we looked, for instance, for WGCNA modules that had been identified to be age-related within the global WGCNA in these subnetworks. The AutoAnnotate Cytoscape plug-in (v1.3) [81] was used to annotate the subnetworks using the clustering algorithm 'Markov Cluster' (MCL) [82] to define and visualize sub-clusters, and the labeling algorithm 'Adjacent Words' to label the sub-clusters. The Cytoscape plug-in BiNGO (v3.0.3) [83] was used for GO enrichment analysis. The p-values of the GO enrichment analysis were adjusted for multiple testing using the FDR approach [84]. Subnetworks were graphically processed with Inkscape (v0.91, www.inkscape.org).

Transcript (functional) annotation

Nucleotide and protein sequences were obtained from the draft version of *C. secundus* genome [23,70]. For annotation, the translated transcripts were searched against the Pfam database (Pfam A, release 30) [85] with the software *hmmscan* (option --cut_ga, HMMer v.3.1b2) [86] and against the InterPro database with the software InterProScan (v5.17-56.0) [87]. Additionally, we did a BLASTX search (NCBI BLAST suite v. 2.3.0) [88] with an e-value of $1e^{-05}$ as cut-off against the protein coding sequences of the termite *Zootermopsis nevadensis* (official gene set version 2.2) [89]. To further assist the annotation, we inferred a set of clusters of orthologous sequence groups (COGs) from the official gene sets at the amino acid level of *C. secundus* (draft version) and *D. melanogaster*, and a BLASTP search of *C. secundus* sequences against the protein coding sequences (longest isoforms only) of *D. melanogaster* with a threshold e-value of $1e^{-05}$.

519 To detect possible TEs, transcripts were searched against the Dfam database (v2.0) [90] using
520 nhmmer [91]. A transcript was considered TE related if there was a hit against the Dfam database
521 and the other annotation sources (Pfam, Interpro and BLAST) were not pointing in the direction of
522 a known gene.
523
524 **Gene identification and construction of gene trees**
525 In addition to the functional annotation, we inferred phylogenetic trees for selected transcripts
526 (Supplementary Archive 1, DRYAD, doi available upon acceptance of the manuscript). Following
527 the procedure described in [23], we retrieved protein coding sequences of the respective cluster of
528 orthologous sequence groups (COGs) from OrthoDB v.9.1 [92] for the following species: *D.*
529 *melanogaster* (DMEL), *Apis mellifera* (AMEL), *Cardiocondyla obscurior* (COBS), *Polistes*
530 *canadensis* (PCAN), *Tribolium castaneum* (TCAS), *Z. nevadensis* (ZNEV) and *Blattella germanica*
531 (BGER). COGs were identified using text search by searching for the gene name or IDs of *D.*
532 *melanogaster*. In case Selenocysteine (U) was included in sequences, "U" was replaced by "X" to
533 avoid problems in downstream analyses since many programs cannot handle Selenocysteine
534 properly. Protein sequences of COGs of above listed species were separately aligned with MAFFT
535 (v.7.294b) applying the G-INS-i algorithm and otherwise default options [93]. For each multiple
536 sequence alignment, a profile hidden Markov model (pHMM) was built with hmmbuild (HMMER
537 v.3.1b2) [86]. Then the pHMM was used to search (hmmsearch) for corresponding protein coding
538 sequences in *C. secundus* and *Macrotermes natalensis* to identify orthologous candidate sequences
539 for each COG in both species. For gene (transcript) tree inference, we only kept sequences with a
540 threshold e-value of $\leq 1e^{-40}$. In addition, we annotated all candidate sequences identified in *C.*
541 *secundus* and *M. natalensis* against the Pfam database (Pfam A, release 30) using hmmscan
542 (HMMER v.3.1b2).

To infer phylogenetic gene trees, we merged for each COG the COGs (amino-acid level) of the seven species listed above with the putatively orthologous amino-acid sequences of *C. secundus* and *M. natalensis*. We generated multiple sequence alignments for a total of 29 genes of interest applying MAFFT (G-INS-i, see above). Ambiguously aligned sequence sections were identified with Aliscore (v. 2 [94,95]; settings: -r: 10000000 and otherwise defaults) and removed with Alicut (v. 2.3, https://www.zfmk.de/en/research/research-centres-and-groups/utilities; masked alignments provided as Supplementary Archive S1 (deposited at DRYAD, doi available upon acceptance of the manuscript). Phylogenetic trees were inferred with IQ-TREE (1.7-beta12 [96] for each gene. The best model was selected with the implemented ModelFinder [97] from all available nuclear models implemented in IQ-TREE plus the two protein mixture models LG4M and LG4X [98] based on the Bayesian Information Criterion (BIC). We applied default settings for rates and the number of rate categories. Statistical support was inferred from 2,000 non-parametric bootstrap replicates. Unrooted trees with the bootstrap support mapped were visualized with Seaview (v4.5.4 [99]) and provided in Newick Format with Supplementary Archive S1 at DRYAD (doi available upon acceptance of the manuscript).

Ethics approval and consent to participate

Not applicable

Consent for publication

Not applicable

Competing interests

The authors declare that they have no competing interests.

Availability of data and materials

Raw sequence reads are deposited on NCBI (Bioproject XXX, BioSample Accessions see Additional File 2, Table S1 – Bioproject numbers and BioSample Accessions will be provided when obtained from NCBI). Additional supplementary data are deposited on the Dryad digital repository DRYAD (DOI provided upon acceptance of the final manuscript). For Supplementary Material please contact: judith.korb@biologie.uni-freiburg.de

Funding

This research was supported by the Deutsche Forschungsgemeinschaft by grants to JK (DFG; KO1895/16-1; KO1895/20-1), one within the Research Unit FOR2281.

Contributions

JK designed the study, JK and MMK collected and identified the termite samples, MMK performed all transcriptome analyses, KM helped with gene identification, with data processing and inferred gene trees, JK did survival analysis and supervised the study, all authors wrote the paper.

Acknowledgments

We thank Florentine Schaub for assistance in the field and wet lab, Daniela Schnaiter for termite colony maintenance, Charles Darwin University (Australia), and especially S. Garnett and the Horticulture and Aquaculture team, provided logistic support to collect *C. secundus*. The Parks and Wildlife Commission, Northern Territory, the Department of the Environment, Water, Heritage and the Arts gave permission to collect. Permit numbers 2002 until 2016, export permit numbers: PWS2001_1508, PWS2003_39852, PWS2004_5769, PWS2007_4154, PWS2010_6997, PWS2014_001342, PWS2016_001559; collection permit numbers: 15656, 18310, 26851, 30073,

36401, 51402, 59044. The study was conducted according to the Nagoya protocol. KM thanks Ondrej Hlinka and the CSIRO IM&T HPC Cluster team.

References

1. Jones OR, Scheuerlein A, Salguero-Gómez R, Camarda CG, Schaible R, Casper BB et al. Diversity of ageing across the tree of life. Nature. 2014; 505: 169-173. doi:10.1038/nature12789.

2. Linford NJ, Bilgir C, Ro J, Pletcher SD. Measurement of lifespan in *Drosophila melanogaster*. J Vis Exp. 2013;71. doi:10.3791/50068.

3. Ungvari Z, Ridgway I, Philipp EER, Campbell CM, McQuary P, Chow T, et al. Extreme longevity is associated with increased resistance to oxidative stress in *Arctica islandica*, the longest-living non-colonial animal. J Gerontol A Biol Sci Med Sci. 2011;66:741-50. doi: 10.1093/gerona/glr044.

4. Rose MR. Evolutionary biology of aging. Oxford University Press; 1991; ill.; 25 cm.

5. Keller L, Genoud M. Extraordinary lifespans in ants: a test of evolutionary theories of ageing. Nature. 1997;389:958-60. doi: 10.1038/40130.

6. Keller L. Queen lifespan and colony characteristics in ants and termites. Insectes Soc. 1998;45:235-46.. doi: 10.1007/s000400050084.

7. Toth AL, Sumner S, Jeanne RL. Patterns of longevity across a sociality gradient in vespid wasps. Curr Opin insect Sci. 2016;16:28-35. doi: 10.1016/j.cois.2016.05.006.

8. Korb J, Thorne B. Sociality in Termites. In: Rubenstein DR, Abbot P, editors. Comparative Social Evolution. Cambridge: Cambridge University Press; 2017. p. 124-53. doi: 10.1017/9781107338319.006.

9. Corona M, Velarde RA, Remolina S, Moran-Lauter A, Wang Y, Hughes KA, et al. Vitellogenin, juvenile hormone, insulin signaling, and queen honey bee longevity. Proc Natl Acad Sci U S A. 2007;104:7128-33. doi: 10.1073/pnas.0701909104.

10. Rascon B, Mutti NS, Tolfsen C, Amdam G V. Honey bee life history plasticity: Development, behavior, and aging. In: Flatt T, Heyland A, editors. Mechanisms of Life History Evolution: The Genetics and Physiology of Life History Traits and Trade-Offs. New York: Oxford Univ Press; 2011. p. 253-66.

11. Rodrigues MA, Flatt T. Endocrine uncoupling of the trade-off between reproduction and somatic maintenance in eusocial insects. Curr Opin Insect Sci. 2016;16:1-8. doi: 10.

12. Weitekamp CA, Libbrecht R, Keller L. Genetics and evolution of social behavior in insects. Annu. Rev. Genet. 2017;51:219-39. doi: 10.1146/annurev-genet-120116-024515.

13. Maekawa K, Ishitani K, Gotoh H, CornetteR, Miura T. Juvenile Hormone titre and vitellogenin gene expression related to ovarian development in primary reproductives compared with nymphs and nymphoid reproductives of the termite Reticulitermes speratus. Physiol Entomol. 2010;35:52-8. doi:10.1111/j.1365-3032.2009.00711.x.

14. Korb J. Juvenile Hormone: A Central Regulator of Termite Caste Polyphenism. In: Zayed A, Kent CFBT-A in IP, editors. Genomics, Physiology and Behaviour of Social Insects. Academic Press; 2015. p. 131-61. doi: 10.1016/bs.aiip.2014.12.004.

631 15. Tasaki E, Mitaka Y, Nozaki T, Kobayashi K, Matsuura K, Iuchi Y. High expression of the
632 breast cancer susceptibility gene BRCA1 in long-lived termite kings. Aging (Albany NY).
633 2018;10:2668-83. doi: 10.18632/aging.101578.

634 16. Wu J, Lu L-Y, Yu X. The role of BRCA1 in DNA damage response. Protein Cell.
635 2010;1:117-23. doi: 10.1007/s13238-010-0010-5.

636 17. Tasaki E, Kobayashi K, Matsuura K, Iuchi Y. An Efficient Antioxidant System in a Long-
637 Lived Termite Queen. PLoS One. 2017;12:e0167412. doi: 10.1371/journal.pone.0167412.

638 18. Tasaki E, Kobayashi K, Matsuura K, Iuchi Y. Long-Lived Termite Queens Exhibit High
639 Cu/Zn-Superoxide Dismutase Activity. Oxid Med Cell Longev. 2018;2018:5127251. doi:
640 10.1155/2018/5127251.

641 19. Münch D, Amdam G V, Wolschin F. Ageing in a eusocial insect: molecular and
642 physiological characteristics of life span plasticity in the honey bee. Funct Ecol.
643 2008;22:407-21. doi:10.1111/j.1365-2435.2008.01419.x.

644 20. Lucas ER, Keller L. Ageing and somatic maintenance in social insects. Curr Opin Insect Sci.
645 2014;5:31-6. doi: 10.1016/j.cois.2014.09.009.

646 21. de Verges J, Nehring V. A critical look at proximate causes of social insect senescence:
647 damage accumulation or hyperfunction? Curr Opin Insect Sci. 2016;16:69-75. doi:
648 10.1016/j.cois.2016.05.003.

649 22. Elsner D, Meusemann K., Korb J.Longevity and transposon defense, the case of termite
650 reproductives. Proc Natl Acad Sci U S A. 2018;115:5504-9. doi: 10.1073/pnas.1804046115

651 23. Monroy Kuhn JM, Meusemann K, Korb J. Long live the queen, the king and the commoner?
652 Transcript expression differences between old and young in the termite *Cryptotermes*
653 *secundus*. PLoS One. 2019;14:e0210371. doi: 10.1371/journal.pone.0210371.

654 24. Evans DS, Kapahi P, Hsueh W-C, Kockel L. TOR signaling never gets old: aging, longevity
655 and TORC1 activity. Ageing Res Rev. 2011;10:225-37. doi: 10.1016/j.arr.2010.04.001.

656 25. Partridge L, Alic N, Bjedov I, Piper MD. Ageing in *Drosophila*: the role of the insulin/Igf
657 and TOR signalling network. Exp Gerontol. 2011;46:376-81. doi:
658 10.1016/j.exger.2010.09.003.

659 26. Antikainen H, Driscoll M, Haspel G, Dobrowolski R. TOR-mediated regulation of
660 metabolism in aging. Aging Cell. 2017;16:1219-33. doi: 10.1111/acel.12689.

661 27. Libbrecht R, Corona M, Wende F, Azevedo DO, Serrão, JR, Keller L. Interplay between
662 insulin signaling, juvenile hormone, and vitellogenin regulates maternal effects on
663 polyphenism in ants. Proc Natl Acad Sci U S A. 2013;110:11050-55. doi:
664 10.1073/pnas.1221781110.

665 28. Mutti NS, Dolezal AG, Wolschin F, Mutti JS, Gill KS, Amdam GV. IRS and TOR nutrient-
666 signaling pathways act via uvenile hormone to influence honey bee caste fate. J Experim.
667 Biol. 2011;214:3977-84. doi: 10.1242/jeb.061499.

668 29. Amdam GV, Norberg K, Fondrk MK, Page RE Jr. Reproductive ground plan may mediate
669 colony-level selection effects on individual foraging behavior in honey bees. Proc Natl Acad
670 Sci U S A. 2004;101:11350-55. doi: 10.1073/pnas.0403073101.

671 30. Warner MR, Qiu L, Holmes MJ, Mikheyev AS, Linksvayer TA. Convergent eusocial
672 evolution is based on a shared reproductive groundplan plus lineage-specific plastic genes.
673 Nat. Commun. 2019;10:2651. doi: 10.1038/s41467-019-10546-w.

674 31. Chandra V, Fetter-Pruneda I, Oxley PR, Ritger A, McKenzie S, Libbrecht R, Kronauer
675 DJC.Social regulation of insulin signaling and the evolution of eusociality in ants. Science
676 2018;361:398-402. doi: 10.1126/science.aar5723.

677 32. Kim K, Lee YS, Carthew RW. Conversion of pre-RISC to holo-RISC by Ago2 during
678 assembly of RNAi complexes. RNA. 2007;13:22-9. doi: 10.1261/rna.283207.

679 33. Sabin LR, Zhou R, Gruber JJ, Lukinova N, Bambina S, Berman A, et al. Ars2 regulates both
680 miRNA- and siRNA- dependent silencing and suppresses RNA virus infection in
681 *Drosophila*. Cell. 2009;138:340-51. doi: 10.1016/j.cell.2009.04.045.

682 34. Ivanov DK, Escott-Price V, Ziehm M, Magwire MM, Mackay TFC, Partridge L, et al.
683 Longevity GWAS Using the Drosophila Genetic Reference Panel. J Gerontol A Biol Sci
684 Med Sci. 2015;70:1470-8. doi: 10.1093/gerona/glv047.

685 35. Cooper, GM. Protein Synthesis, Processing, and Regulation (Chapter 7). In: The Cell: A
686 Molecular Approach. 2nd edition. Sunderland, MA: Sinauer Associates; 2000.
687 36. Wong E, Cuervo AM. Integration of clearance mechanisms: the proteasome and autophagy.
688 Cold Spring Harb Perspect Biol. 2010;2:a006734. doi: 10.1101/cshperspect.a006734.
689 37. Putiri EL, Robertson KD. Epigenetic mechanisms and genome stability. Clin Epigenetics.
690 2010;2:299-314. doi:10.1007/s13148-010-0017-z.
691 38. Gozani O, Shi Y. Histone Methylation in Chromatin Signaling BT - Fundamentals of
692 Chromatin. In: Workman JL, Abmayr SM, editors. New York, NY: Springer New York;
693 2014. p. 213-56. doi:10.1007/978-1-4614-8624-4_5.

694 39. Steunou A-L, Rossetto D, Côté J. Regulating Chromatin by Histone Acetylation BT -
695 Fundamentals of Chromatin. In: Workman JL, Abmayr SM, editors. New York, NY:
696 Springer New York; 2014. p. 147-212. doi:10.1007/978-1-4614-8624-4_4.

40. Plongthongkum N, Kullawong N, Panyim S, Tirasophon W. Ire1 regulated XBP1 mRNA splicing is essential for the unfolded protein response (UPR) in Drosophila melanogaster. Biochem Biophys Res Commun. 2007;354:789-94.

41. Remondelli P, Renna M. The Endoplasmic Reticulum Unfolded Protein Response in Neurodegenerative Disorders and Its Potential Therapeutic Significance. Front Mol Neurosci. 2017;10:187. doi:10.3389/fnmol.2017.00187.

42. Gorrini C, Baniasadi PS, Harris IS, Silvester J, Inoue S, Snow B, et al. BRCA1 interacts with Nrf2 to regulate antioxidant signaling and cell survival. J Exp Med. 2013;210:1529-44. doi: 10.1084/jem.20121337.

43. Piatek MJ, Werner A. Endogenous siRNAs: regulators of internal affairs. Biochem Soc Trans. 2014;42:1174-9. doi:10.1042/BST20140068.

44. Dang W, Steffen KK, Perry R, Dorsey JA, Johnson FB, Shilatifard A, et al. Histone H4 lysine 16 acetylation regulates cellular lifespan. Nature. 2009;459:802-7. doi: 10.1038/nature08085.

45. Wood JG, Hillenmeyer S, Lawrence C, Chang C, Hosier S, Lightfoot W, et al. Chromatin remodeling in the aging genome of Drosophila. Aging Cell. 2010;9:971-8.. doi: 10.1111/j.1474-9726.2010.00624.x.

46. Larson K, Yan S-J, Tsurumi A, Liu J, Zhou J, Gaur K, et al. Heterochromatin formation promotes longevity and represses ribosomal RNA synthesis. PLoS Genet. 2012;8:e1002473. doi: 10.1371/journal.pgen.1002473.

47. Wood JG, Helfand SL. Chromatin structure and transposable elements in organismal aging. Front Genet. 2013;4:274. doi: 10.3389/fgene.2013.00274.

719 48. Chen H, Zheng X, Xiao D, Zheng Y. Age□associated de□repression of retrotransposons in
720 the *Drosophila* fat body, its potential cause and consequence. Aging Cell. 2016;15:542-52.
721 doi:10.1111/acel.12465.

722 49. Wood JG, Jones BC, Jiang N, Chang C, Hosier S, Wickremesinghe P, et al. Chromatin-
723 modifying genetic interventions suppress age-associated transposable element activation and
724 extend life span in *Drosophila*. Proc Natl Acad Sci U S A. 2016;113:11277-82 doi:
725 10.1073/pnas.1604621113.

726 50. Liu Y, Ye X, Jiang F, Liang C, Chen D, Peng J, et al. C3PO, an endoribonuclease that
727 promotes RNAi by facilitating RISC activation. Science. 2009;325:750-3. doi:
728 10.1126/science.1176325.

729 51. Kandasamy SK, Zhu L, Fukunaga R. The C-terminal dsRNA-binding domain of Drosophila
730 Dicer-2 is crucial for efficient and high-fidelity production of siRNA and loading of siRNA
731 to Argonaute2. RNA. 2017;23:1139-53. doi: 10.1261/rna.059915.116.

732 52. Tsuboyama K, Tadakuma H, Tomari Y. Conformational activation of Argonaute by distinct
733 yet coordinated actions of the Hsp70 and Hsp90 chaperone systems. Mol Cell. 2018;70:722-
734 729.e4. doi: 10.1016/j.molcel.2018.04.010.

735 53. Liu Y, Beyer A, Aebersold R. On the dependency of cellular protein levels on mRNA
736 abundance. Cell. 2016;165:535-50. doi: 10.1016/j.cell.2016.03.014.

737 54. Cao JQ, Tong WS, Yu HY, Tobe SS, Bendena WG, Hui JHL. Chapter Three - The Role of
738 MicroRNAs in Drosophila Regulation of Insulin-Like Peptides and Ecdysteroid Signalling:
739 Where Are We Now? In: Verlinden HBT-A in IP, editor. Insect Epigenetics. Academic
740 Press; 2017. p. 55-85. doi: 10.1016/bs.aiip.2017.02.002.

741 55. Laplante M, Sabatini DM. mTOR signaling at a glance. J Cell Sci. 2009;122 Pt 20:3589-94.
742 doi: 10.1242/jcs.051011.

743 56. Zhao J, Zhai B, Gygi SP, Goldberg AL. mTOR inhibition activates overall protein
744 degradation by the ubiquitin proteasome system as well as by autophagy. Proc Natl Acad
745 Sci U S A. 2015;112:15790-7. doi: 10.1073/pnas.1521919112.

746 57. Ichimura Y, Waguri S, Sou Y-S, Kageyama S, Hasegawa J, Ishimura R, et al.
747 Phosphorylation of p62 activates the Keap1-Nrf2 pathway during selective autophagy. Mol
748 Cell. 2013;51:618-31. doi: 10.1016/j.molcel.2013.08.003.

749 58. Aramburu J, Ortells MC, Tejedor S, Buxade M, Lopez-Rodriguez C. Transcriptional
750 regulation of the stress response by mTOR. Sci Signal. 2014;7:re2. doi:
751 10.1126/scisignal.2005326.

752 59. Tsakiri EN, Sykiotis GP, Papassideri IS, Terpos E, Dimopoulos MA, Gorgoulis VG, et al.
753 Proteasome dysfunction in Drosophila signals to an Nrf2-dependent regulatory circuit
754 aiming to restore proteostasis and prevent premature aging. Aging Cell. 2013;12:802-13.
755 doi: 10.1111/acel.12111.

756 60. Sykiotis GP, Bohmann D. Keap1/Nrf2 signaling regulates oxidative stress tolerance and
757 lifespan in Drosophila. Dev Cell. 2008;14:76-85. doi: 10.1016/j.devcel.2007.12.002.

758 61. Tullet JMA, Hertweck M, An JH, Baker J, Hwang JY, Liu S, et al. Direct inhibition of the
759 longevity-promoting factor SKN-1 by insulin-like signaling in C. elegans. Cell.
760 2008;132:1025-38. doi: 10.1016/j.cell.2008.01.030.

761 62. Tolfsen CC, Baker N, Kreibisch C, Amdam GV. Flight restriction prevents associative
762 learning deficits but no changes in brain protein-adduct formation during honeybee ageing .
763 J Exp Biol. 2011;214:1322-32.

764 63. Parker JD, Parker KM, Sohal BH, Sohal RS, Keller L. Decreased expression of Cu-Zn
765 superoxide dismutase 1 in ants with extreme lifespan. Proc Natl Acad Sci U S A.
766 2004;101:3486-9. doi:10.1073/pnas.0400222101.

767 64. Heinze J, Schrempf A. Terminal investment: individual reproduction of ant queens increases
768 with age. PLoS One. 2012;7:e35201. doi: 10.1371/journal.pone.0035201.

769 65. Korb J, Lenz M. Reproductive decision-making in the termite, Cryptotermes secundus
770 (Kalotermitidae), under variable food conditions. Behav Ecol. 2004;15:390-5. doi:
771 10.1093/beheco/arh033.

772 66. Korb J, Katrantzis S. Influence of environmental conditions on the expression of the sexual
773 dispersal phenotype in a lower termite: implications for the evolution of workers in termites.
774 Evol Dev. 2004;6:342-52. doi: 10.1111/j.1525-142X.2004.04042.x.

775 67. IBM Corp. Released 2015. IBM SPSS Statistics for Windows, Version 23.0. Armonk, NY:
776 IBM Corp.

777 68. Andrews S. FastQC: a quality control tool for high throughput sequence data. 2010.
778 http://www.bioinformatics.babraham.ac.uk/projects/fastqc.

779 69. Bray NL, Pimentel H, Melsted P, Pachter L. Near-optimal probabilistic RNA-seq
780 quantification. Nat Biotech. 2016;34:525-7. doi:10.1038/nbt.3519.

781 70. Harrison MC, Jongepier E, Robertson HM, Arning N, Bitard-Feildel T, Chao H, et al.
782 Hemimetabolous genomes reveal molecular basis of termite eusociality. Nat Ecol Evol.
783 2018;2:557-66. doi: 10.1038/s41559-017-0459-1.

784 71. Love MI, Huber W, Anders S. Moderated estimation of fold change and dispersion for
785 RNA-seq data with DESeq2. Genome Biol. 2014;15:550. doi: 10.1186/s13059-014-0550-8.

786 72. R Core Team. 2018 R: A Language and Environment for Statistical Computing (R
787 Foundation for Statistical Computing, Vienna). https://www.R-project.org/.

788 73. Nueda MJ, Martorell-Marugan J, Marti C, Tarazona S, Conesa A. Identification and
789 visualization of differential isoform expression in RNA-seq time series. Bioinformatics.
790 2018;34:524-6. doi: 10.1093/bioinformatics/btx578.

791 74. Nueda MJ, Tarazona S, Conesa A. Next maSigPro: updating maSigPro bioconductor
792 package for RNA-seq time series. Bioinformatics. 2014;30:2598-602.
793 doi:10.1093/bioinformatics/btu333.

794 75. Langfelder P, Horvath S. WGCNA: an R package for weighted correlation network analysis.
795 BMC Bioinformatics. 2008;9:559. doi:10.1186/1471-2105-9-559.

796 76. Zhang B, Horvath S. A general framework for weighted gene co-expression network
797 analysis. Stat Appl Genet Mol Biol. 2005;4:Article17. doi: 10.2202/1544-6115.1128.

798 77. Horvath S, Dong J. Geometric interpretation of gene coexpression network analysis. PLoS
799 Comput Biol. 2008;4:e1000117. doi: 10.1371/journal.pcbi.1000117.

800 78. Yip AM, Horvath S. Gene network interconnectedness and the generalized topological
801 overlap measure. BMC Bioinformatics. 2007;8:22. doi:10.1186/1471-2105-8-22.

802 79. Langfelder P, Zhang B, Horvath S. Defining clusters from a hierarchical cluster tree: the
803 Dynamic Tree Cut package for R. Bioinformatics. 2008;24:719-20. doi:
804 10.1093/bioinformatics/btm563.

805 80. Shannon P, Markiel A, Ozier O, Baliga NS, Wang JT, Ramage D, et al. Cytoscape: a
806 software environment for integrated models of biomolecular interaction networks. Genome
807 Res. 2003;13:2498-504. doi: 10.1101/gr.1239303.

808 81. Kucera M, Isserlin R, Arkhangorodsky A, Bader GD. AutoAnnotate: A Cytoscape app for
809 summarizing networks with semantic annotations. F1000Research. 2016;5:1717.
810 doi:10.12688/f1000research.9090.1.

811 82. Enright AJ, Van Dongen S, Ouzounis CA. An efficient algorithm for large-scale detection of
812 protein families. Nucleic Acids Res. 2002;30:1575-84.

813 83. Maere S, Heymans K, Kuiper M. BiNGO: a Cytoscape plugin to assess overrepresentation
814 of Gene Ontology categories in Biological Networks. Bioinformatics. 2005;21:3448-9. doi:
815 10.1093/bioinformatics/bti551.

816 84. Benjamini Y, Hochberg Y. Controlling the False Discovery Rate: A Practical and Powerful
817 Approach to Multiple Testing. J R Stat Soc Ser B. 1995;57:289-300.
818 http://www.jstor.org/stable/2346101.

819 85. Finn RD, Coggill P, Eberhardt RY, Eddy SR, Mistry J, Mitchell AL, et al. The Pfam protein
820 families database: towards a more sustainable future. Nucleic Acids Res. 2016;44:D279-85.
821 doi: 10.1093/nar/gkv1344.

822 86. Eddy SR. Accelerated Profile HMM Searches. PLoS Comput Biol. 2011;7:e1002195. doi:
823 10.1371/journal.pcbi.1002195.

824 87. Jones P, Binns D, Chang H-Y, Fraser M, Li W, McAnulla C, et al. InterProScan 5: genome-
825 scale protein function classification. Bioinformatics. 2014;30:1236-40. doi:
826 10.1093/bioinformatics/btu031.

827 88. Altschul SF, Gish W, Miller W, Myers EW, Lipman DJ. Basic local alignment search tool. J
828 Mol Biol. 1990;215:403-10. doi: 10.1016/S0022-2836(05)80360-2.

829 89. Terrapon N, Li C, Robertson HM, Ji L, Meng X, Booth W, et al. Molecular traces of
830 alternative social organization in a termite genome. Nat Commun. 2014;5:3636. doi:
831 10.1038/ncomms4636.

832 90. Hubley R, Finn RD, Clements J, Eddy SR, Jones TA, Bao W, et al. The Dfam database of
833 repetitive DNA families. Nucleic Acids Res. 2016;44:D81-9. doi: 10.1093/nar/gkv1272.

834 91. Wheeler TJ, Eddy SR. nhmmer: DNA homology search with profile HMMs.
835 Bioinformatics. 2013;29:2487-9. doi: 10.1093/bioinformatics/btt403.

836 92. Zdobnov EM, Tegenfeldt F, Kuznetsov D, Waterhouse RM, Simao FA, Ioannidis P, et al.
837 OrthoDB v9.1: cataloging evolutionary and functional annotations for animal, fungal, plant,
838 archaeal, bacterial and viral orthologs. Nucleic Acids Res. 2017;45:D744-9. doi:
839 10.1093/nar/gkw1119.

840 93. Katoh K, Standley DM. MAFFT multiple sequence alignment software version 7:
841 improvements in performance and usability. Mol Biol Evol. 2013;30:772-80.
842 doi:10.1093/molbev/mst010-

843 94. Misof B, Misof K. A Monte Carlo approach successfully identifies randomness in multiple
844 sequence alignments: a more objective means of data exclusion. Syst Biol. 2009;58:21-34.
845 doi: 10.1093/sysbio/syp006.

846 95. Kück P, Meusemann K, Dambach J, Thormann B, von Reumont BM, Wägele JW et al.
847 Parametric and non-parametric masking of randomness in sequence alignments can be
848 improved and leads to better resolved trees. Front Zool. 2010;7:10. doi: 10.1186/1742-9994-
849 7-10.

850 96. Nguyen L-T, Schmidt HA, Von Haeseler A, Minh BQ. IQ-TREE: a fast and effective
851 stochastic algorithm for estimating maximum-likelihood phylogenies. Mol Biol Evol.

852 2015;32:268-74. doi: 10.1093/molbev/msu300.

853 97. Kalyaanamoorthy S, Minh BQ, Wong TKF, von Haeseler A, Jermiin LS. ModelFinder: fast
854 model selection for accurate phylogenetic estimates. Nat Methods. 2017;14:587-9. doi:
855 10.1038/nmeth.4285.

856 98. Le SQ, Dang CC, Gascuel O. Modeling protein evolution with several amino acid
857 replacement matrices depending on site rates. Mol Biol Evol. 2012;29:2921-36. doi:
858 10.1093/molbev/mss112

859 99. Gouy M, Guindon S, Gascuel O. SeaView version 4: A multiplatform graphical user
860 interface for sequence alignment and phylogenetic tree building. Mol Biol Evol.
861 2010;27:221-4. doi: 10.1093/molbev/msp259.

FIGURE LEGENDS

Figure 1. Survival plot of *C. secundus* queens.

Shown is the age-dependent survival probability of queens. The median longevity of queens in the laboratory after successful colony establishment was estimated with Kaplan Meier survival analysis to be 12 years (mean longevity: 11.1 years). The maximum lifespan was 13 years. After an age of around 11 years, life expectancy declines rapidly; out of eight queens with a potential age ≥ 12 years, all had died, except one 13-year old queen.

Figure 2. Median expression profiles of DETs assigned to Iso-MaSigPro clusters.

Iso-MaSigPro grouped the differentially expressed transcripts (DETs) into six clusters. DETs of cluster 1, 4 and 6 were especially highly expressed in old queens, while those of cluster 3 and 5 characterized middle-aged queens and those of cluster 2 young queens. The expression values correspond to normalized counts (see Methods). The youngest queen (age: 2 years) was taken as time step zero and each of the subsequent older queens (based on chronological age) were considered to be one time step older. One age class (time step 8; age: 10 years) consisted of two samples.

Figure 3. Young subnetwork highlighting Iso-MaSigPro DETs.

Shown is WGCNA-based co-expression network of transcripts, which contains DETs characterising young and middle-aged queens and their one- and two-step neighbors (*i.e.*, young subnetwork; for more information, see text and Additional File 1, Figure S1 and S2). Highlighted are the Iso-MaSigPro DETs of cluster 2, 3, and 5, characterizing young and middle-aged queens (see insert; Fig. 2). Node colors correspond to the WGCNA modules. Transposable element (TE) related transcripts are highlighted with a '?'. Transcripts with an asterisk indicate 1:1 orthologs (*C.*

886 *secundus* and *D. melanogaster*). Connection length and width do not have a meaning. Red circles
887 indicate transcripts discussed in the text.
888
889 **Figure 4. Genes related to protein synthesis that were found in the old subnetwork.**
890 Shown are genes that have been related to various processes of protein synthesis, from initiation,
891 and elongation to termination. For all genes listed, corresponding transcripts were present in the old
892 subnetwork of *C. secundus* queens. Figure modified after [35].
893
894 **Figure 5. Genes related to the proteasome complex that were found in the old subnetwork.**
895 Shown are genes that have been related to the proteasome complex. The textbox in red indicates
896 subunits, for which we found transcripts in the old subnetwork. Figure modified after [36].
897
898 **Figure 6. Transcription- and proteostasis-related expression pattern in old *Cryptotermes***
899 ***secundus* queens**.
900 Depicted is the expression patterns of genes related to transcription and proteostasis for old *C.*
901 *secundus* queens (red arrows) in contrast to that reported for other species (grey arrows). Old *C.*
902 *secundus* queens were characterized by a very strong proteostasis signal indicative of an
903 upregulation of protein degradation, together with protein synthesis and protein folding. This is
904 unusual because old organisms are typically characterized by a downregulation of these processes.
905 The simultaneous activation of protein synthesis and degradation in old *C. secundus* queens can be
906 explained by the activity of the transcription factor cnc/Nrf-2 (for more details, see text). The inner
907 cycle arrows depict the protein life cycle; dashed arrows indicate the special case when mistakes/
908 errors occur. After a protein is degraded, its components are recycled.
909

Figure 7. Aging signal of *C. secundus* queens in relation to known aging pathways.

Shown are simplified IIS (insulin/insulin-like growth factor signaling; blue), TOR (target of rapamycin; green), and ecdysone (brown) pathways and their interactions with an emphasis on **A.** ecdysone biosynthesis and **B.** protein synthesis and degradation. Red encircled genes were members of the old subnetwork, and thus highly expressed in old queens. Important genes that regulate protein synthesis and degradation are depicted in white. In short, the TOR pathway controls cell growth and metabolism in response to amino acid availability. It is generally composed of two main complexes: TORC1 and TORC2 [55]. Activation of TORC1 promotes mRNA translation, for instance, via S6K /eIF4B / eIF-4a and 4E-BP / eIF4E. Additionally, active TORC1 inhibits autophagy by targeting upstream components necessary for autophagy activation, like Atg1. TOR interacts with IIS, which also regulates multiple physiological functions, including aging. Generally, an active IIS pathway can activate the TORC1 complex via phosphorylation and inactivation of Tsc2 by AKT. AKT inhibits the transcription factor foxo via phosphorylation, which results in the inhibition of transcription of many downstream genes, e.g. involved in lifespan extension, stress response and autophagy. Stress induced *Cnc* can activate TORC1 in a positive feedback loop (big dashed arrow). It may be responsible for the simultaneous upregulation of protein synthesis and degradation. For more information, see text. Figures are adapted after [53-55].

Additional Files

Additional File 1 (Additional_File_1.pdf): Supplementary Figures S1-S10.

Figure S1: Schematic workflow. Details are explained in the Methods.

Figure S2: WGCNA modules of co-expressed transcripts that negatively correlate with age. Modules marked with an asterisk were found in the young subnetwork. Modules are named after colors by WGCNA.

Figure S3: WGCNA modules of co-expressed transcripts that positively correlate with age. Modules marked with an asterisk were found in the old subnetwork. Modules are named after colors by WGCNA.

Figure S4: GO enrichment for the WGCNA module 'tan' that positively correlated with age and which had many old-age DETs. Details are shown for BP (Biological Process), which revealed an enrichment of transcripts for ribosomal and tRNA related functions.

Figure S5: Young and old transcript subnetworks corresponding to the second level neighborhood of Iso-MaSigPro DETs. Age-related DETs were located in the WGCNA co-expression network and these DETs and their one- and two-step neighbors (*i.e.*, the 'second level neighborhood') were then extracted from the co-expression network to provide the shown networks.

Figure S6: BiNGO GO enrichment (Biological Process) for the young subnetwork. No terms were significantly enriched after correcting for multiple testing (FDR).

Figure S7: BiNGO GO enrichment (Biological Process) for the old subnetwork. Colored nodes are GO terms that were significantly enriched after correcting for multiple testing (FDR).

Figure S8: BiNGO GO enrichment of (Molecular Function; Cellular Component) for the old subnetwork. Colored nodes are GO terms that were significantly enriched after correcting for multiple testing (FDR).

952 Figure S9: BiNGO GO enrichment (Biological Process; Molecular Function; Cellular Component)
953 for the 'green' WGCNA module, which is part of the old subnetwork. Colored nodes are GO terms
954 that were significantly enriched after correcting for multiple testing (FDR).
955 Figure S10: BiNGO GO enrichment (Biological Process, Molecular Function; Cellular Component)
956 for the 'paleturquoise' WGCNA module, which is part of the old subnetwork. Nodes in color are
957 GO terms significantly enriched after correcting for multiple testing (FDR).
958
959 **Additional File 2 (Additional_File_2.xlsx): Supplementary Tables S1-S4.**
960 Table S1: Sample information of samples included in this study.
961 Table S2: Differentially expressed transcripts of the Iso-MaSigPro analysis, separately for cluster 1-
962 6.
963 Table S3. Transcripts in the young subnetwork (SNW).
964 Transcripts in the young subnetwork (SNW) classified into major categories; TE-related transcripts
965 of the young subnetwork (SNW).
966 Table S4. Transcripts in the old subnetwork (SNW).
967 Transcripts in the old subnetwork (SNW) classified into major categories; TE-related transcripts of
968 the old subnetwork (SNW).
969
970 **Additional File 3 (Additional_File_3.pdf)**
971 WGCNA module-age associations. Listed are the eigengene values for each module.
972
973 **Additional File 4 (Additional_File_4.xlsx): Supplementary Table S5.**
974 Go terms for enriched differentially expressed transcripts (DETs) included in BiNGO module
975 green; BiNGO module paleturquoise; BiNGO module tan; BiNGO module Thistle2; BiNGO

976 module snow; BiNGO module cyan; BiNGO module deeppink1; BiNGO module navajowhite;
977 BiNGO module blue2_NS; BiNGO module cornflowerblue_NS; BiNGO module pink3_NS;
978 BiNGO module steelblue4_NS.
979

980 Supplementary Archive 1

981 The Supplementary Archive includes i) masked multiple sequence alignments (MSAs) of 29
982 selected genes (subdirectory “MSAs” used for ML gene tree inference in FASTA format) in IQ-
983 TREE and ii) inferred ML gene trees (subdirectory “ML_gene_trees” in NEWICK format) for each
984 of the 29 genes including non-parametric statistical bootstrap support. These gene trees additionally
985 helped to ensure a proper assignment of transcripts to repective genes.

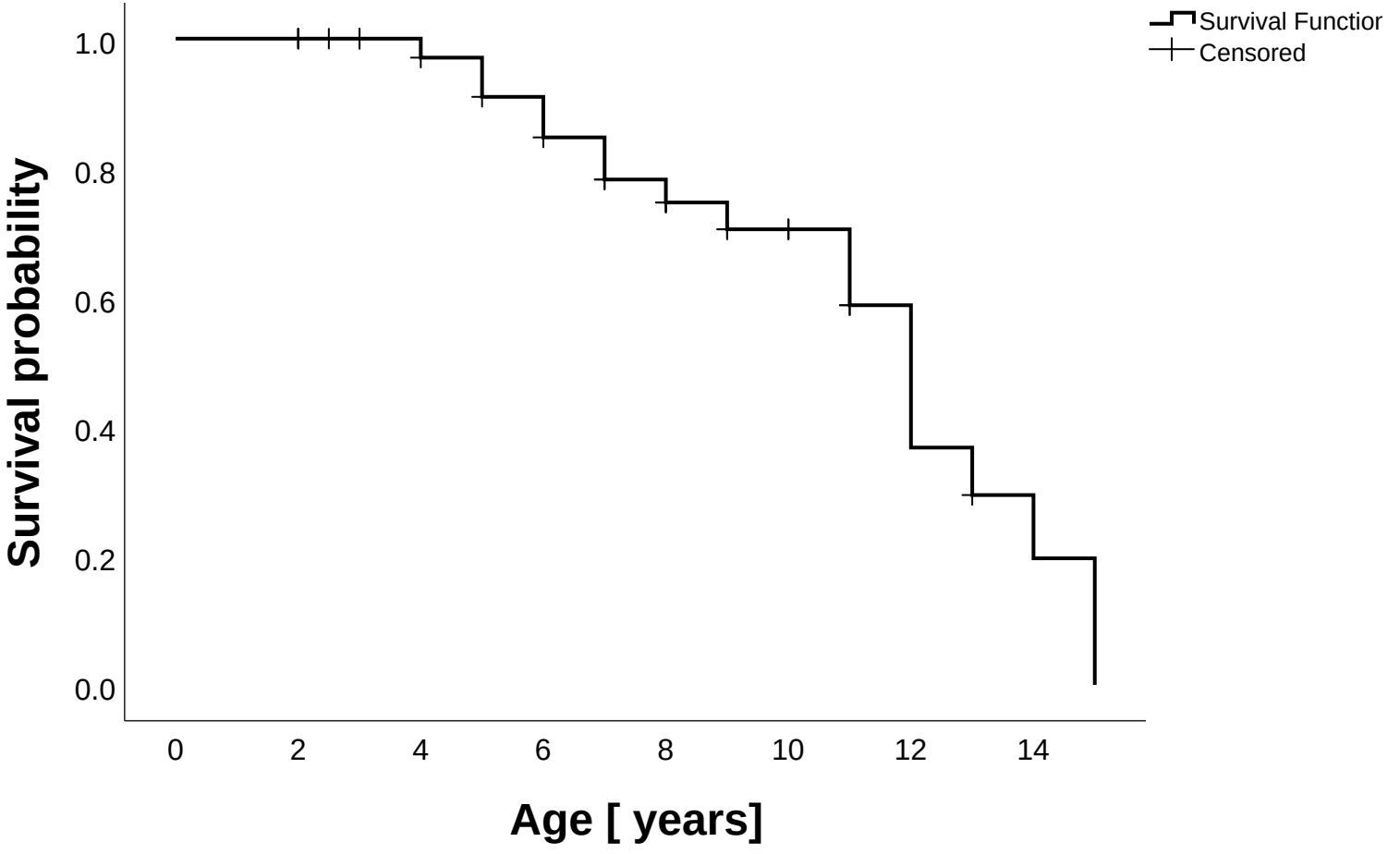
Survival Functior
Censored
Survival probability
1.0
0.8
0.6
0.4
0.2
0.0
0
2
4
6
8
10
12
14
Age [years]

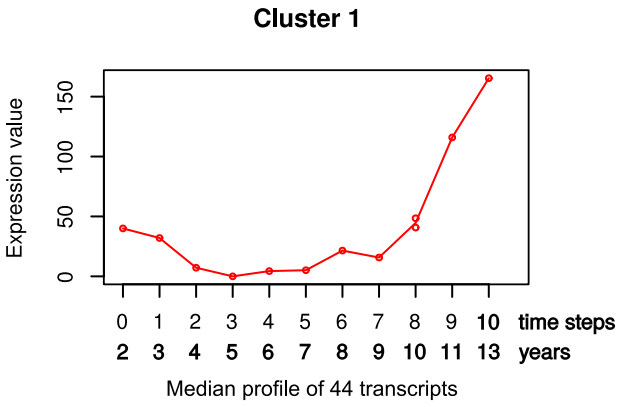
Cluster 1
Expression value
0
50
100
150
0 1 2 3 4 5 6 7 8 9 10 time steps
2 3 4 5 6 7 8 9 10 11 13 years
Median profile of 44 transcripts

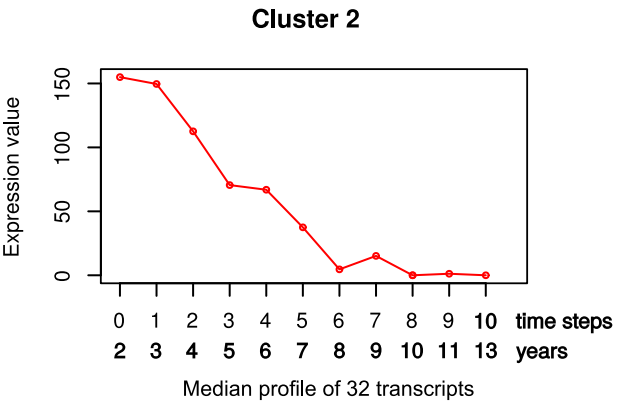
Cluster 2
Expression value
0
50
100
150
0 1 2 3 4 5 6 7 8 9 10 time steps
2 3 4 5 6 7 8 9 10 11 13 years
Median profile of 32 transcripts

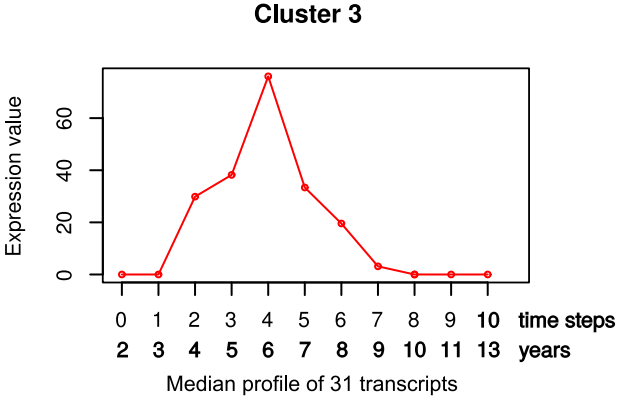
Cluster 3
Expression value
0
20
40
60
0 1 2 3 4 5 6 7 8 9 10 time steps
2 3 4 5 6 7 8 9 10 11 13 years
Median profile of 31 transcripts

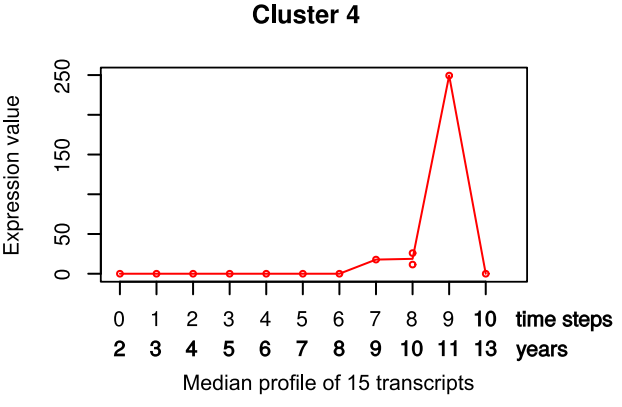
Cluster 4
Expression value
0
50
150
250
0 1 2 3 4 5 6 7 8 9 10 time steps
2 3 4 5 6 7 8 9 10 11 13 years
Median profile of 15 transcripts

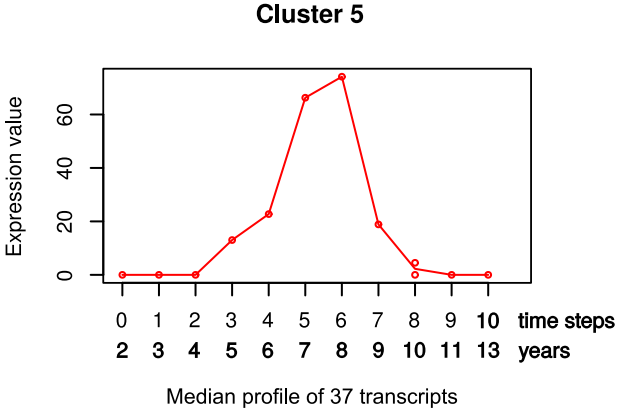
Cluster 5
Expression value
0
20
40
60
0 1 2 3 4 5 6 7 8 9 10 time steps
2 3 4 5 6 7 8 9 10 11 13 years
Median profile of 37 transcripts

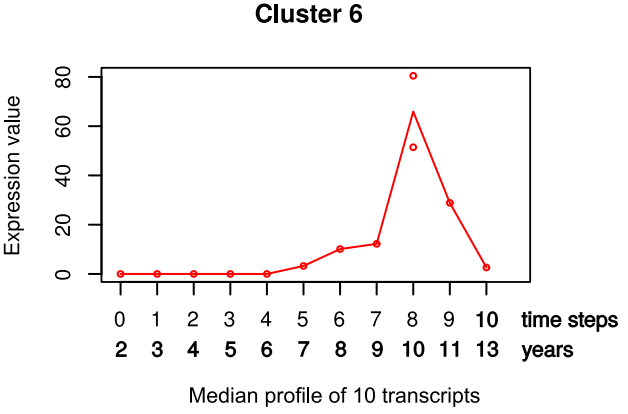
Cluster 6
Expression value
0
20
40
60
80
0 1 2 3 4 5 6 7 8 9 10 time steps
2 3 4 5 6 7 8 9 10 11 13 years
Median profile of 10 transcripts

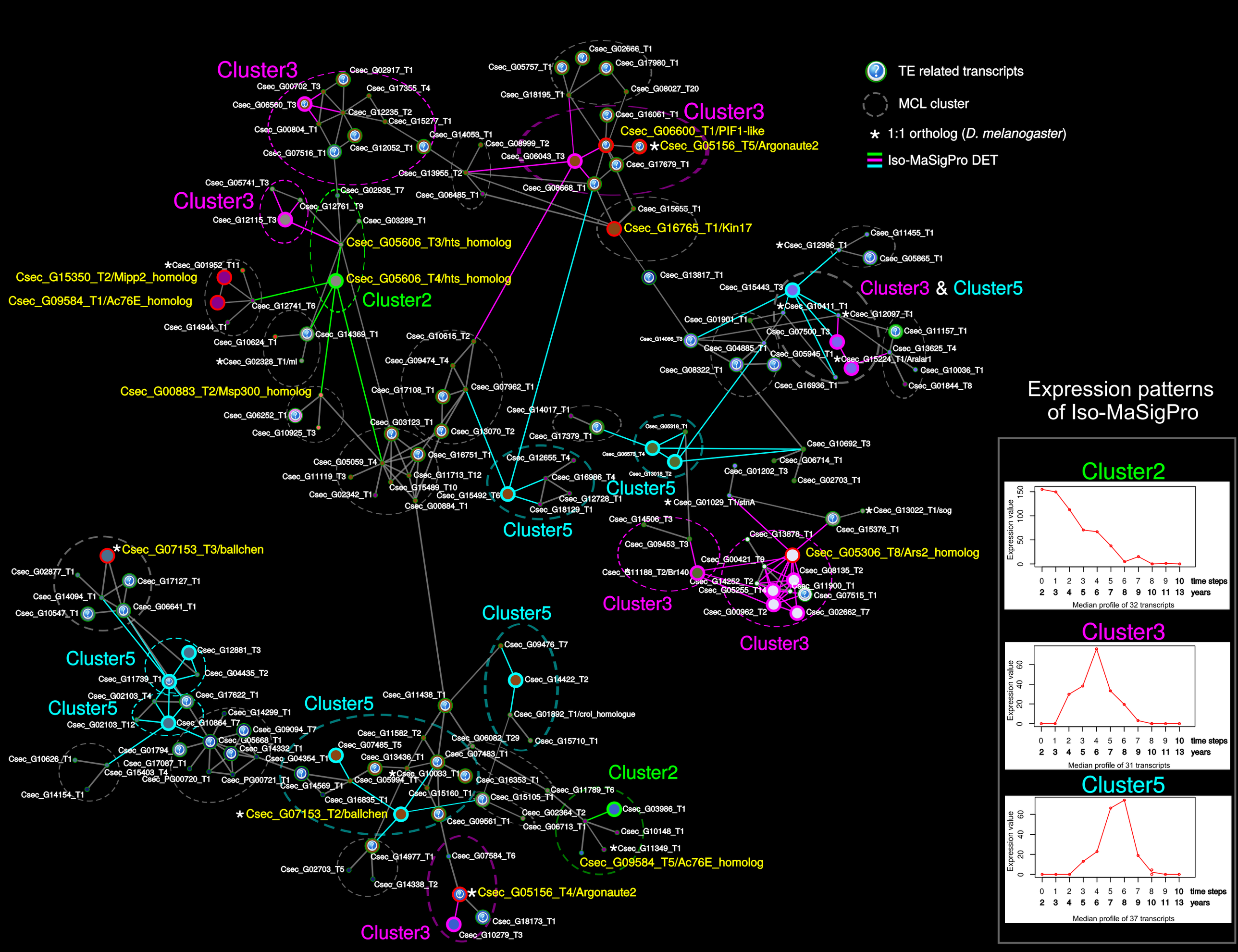
TE related transcripts
MCL cluster
★ 1:1 ortholog (D. melanogaster)
Iso-MaSigPro DET
Expression patterns of Iso-MaSigPro
Cluster2
Cluster3
Cluster5
Expression value
time steps
years
Median profile of 32 transcripts
Median profile of 31 transcripts
Median profile of 37 transcripts
Csec_G05606_T3/hts_homolog
Csec_G05606_T4/hts_homolog
Csec_G16765_T1/Kin17
Csec_G06600_T1/PIF1-like
★Csec_G05156_T5/Argonaute2
Csec_G15350_T2/Mipp2_homolog
Csec_G09584_T1/Ac76E_homolog
Csec_G00883_T2/Msp300_homolog
★Csec_G07153_T3/ballchen
Csec_G05306_T8/Ars2_homolog
★Csec_G07153_T2/ballchen
Csec_G09584_T5/Ac76E_homolog
★Csec_G05156_T4/Argonaute2

Initiation

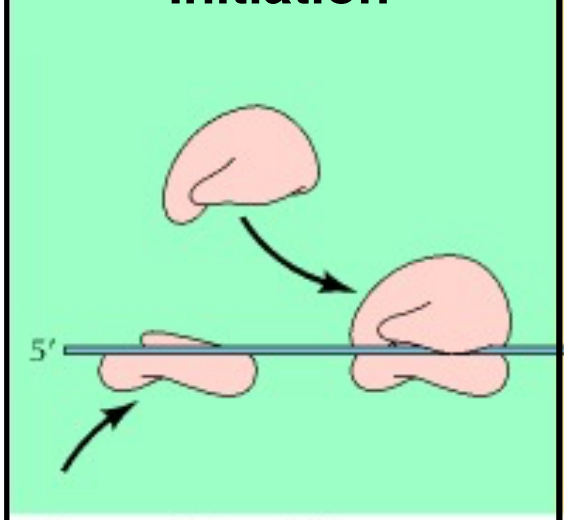

Ribosome binds mRNA at start codon

eIF3h
eIF3f1
eIF2A
eIF4A
eIF3c
eIF4B
eIF3l
eIF1
eIF5B
eIF2gamma
eIF2beta
eIF3k
eIF3d1
eIF3i
eIF2Bepsilon
eIF2alpha

eIF3j
eIF6
eIF4G1

Elongation

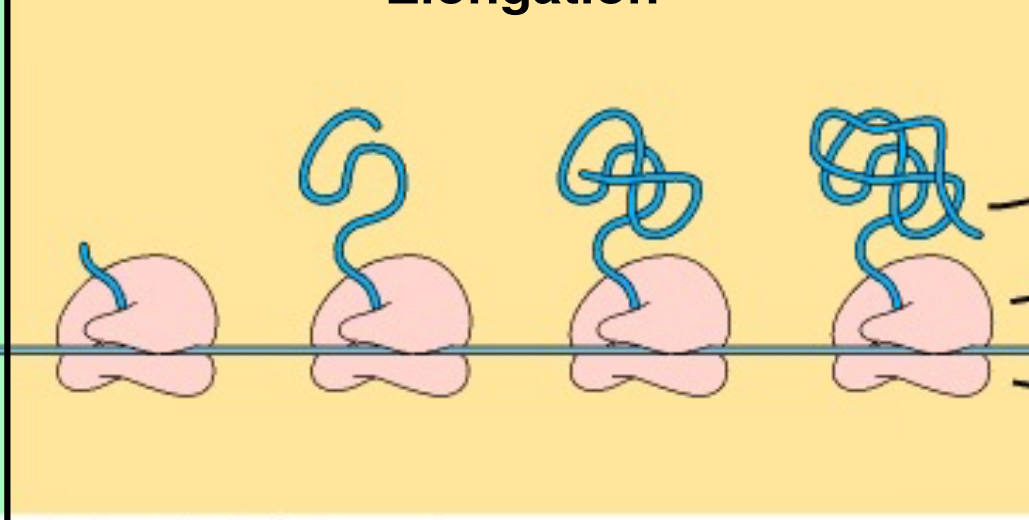

Polypeptide chain elongates by successively adding amino acids

eEF1gamma
eEF1beta
eEF1beta
eEF1delta

Termination

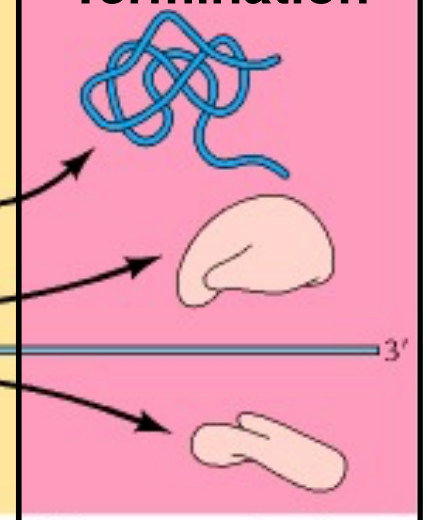

When a stop codon is encountered, polypeptide is released and ribosome dissociates

eRF3

Ribosomal proteins

RpL28
RpL18A
RpS26
RpL40
RpLP0-like
RpL23
RpL27
RpL34a
RpL36A
RpS30

RpL24-like
RpS3A
RpL4
RpL5
RpL23A
RpLP0
RpS15Aa
RpL18
RpL19
RpL8

RpLP1
RpS25
RpS18
RpL22
RpS9
RpL27A
RpL10
RpL36
RpL26
RpS23

RpS13
RpS15
RpL6 (3)
RpS17

Aminoacyl-tRNA Synthetases

GluProRS
CysRS
IleRS
AsnRS
GlnRS
alpha-PheRS

ThrRS
LysRS
HisRS
GlyRS
ValRS
beta-PheRS
AsnRS

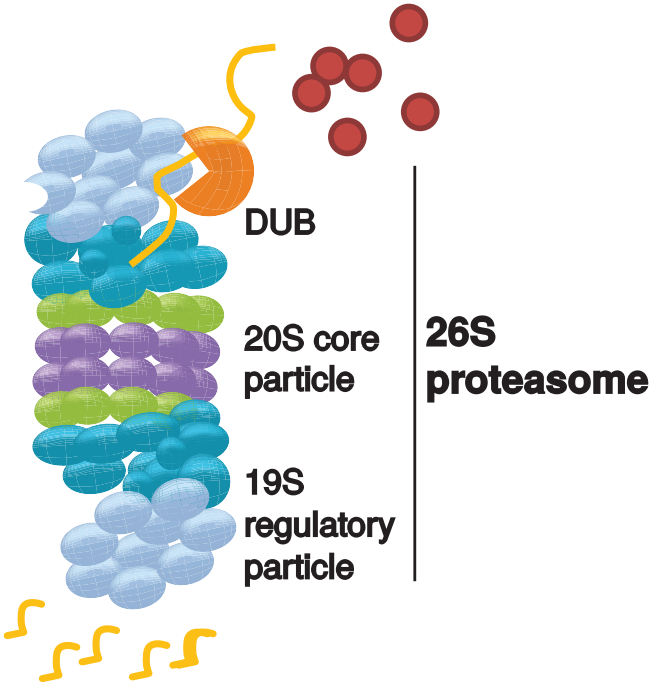

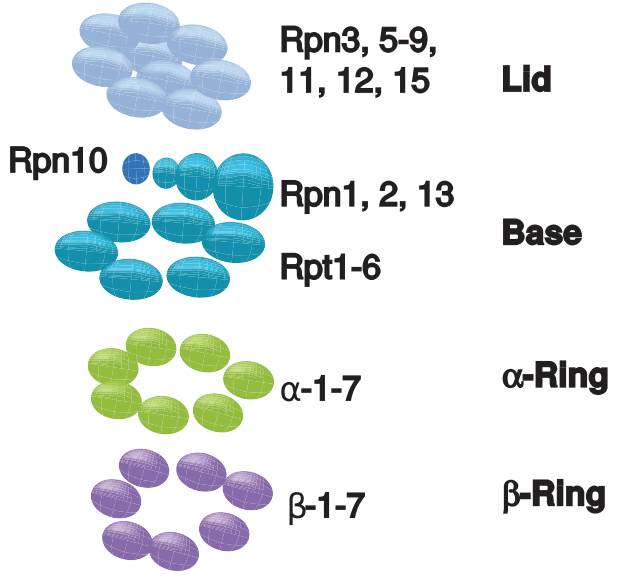

Subunits in the "old" subnetwork

Rpn3, 7, 8, 9, 11, 12

Rpn2, 10(2)
Rpt1, 2, 3, 4, 5

3, 4, 5, 7

1-7

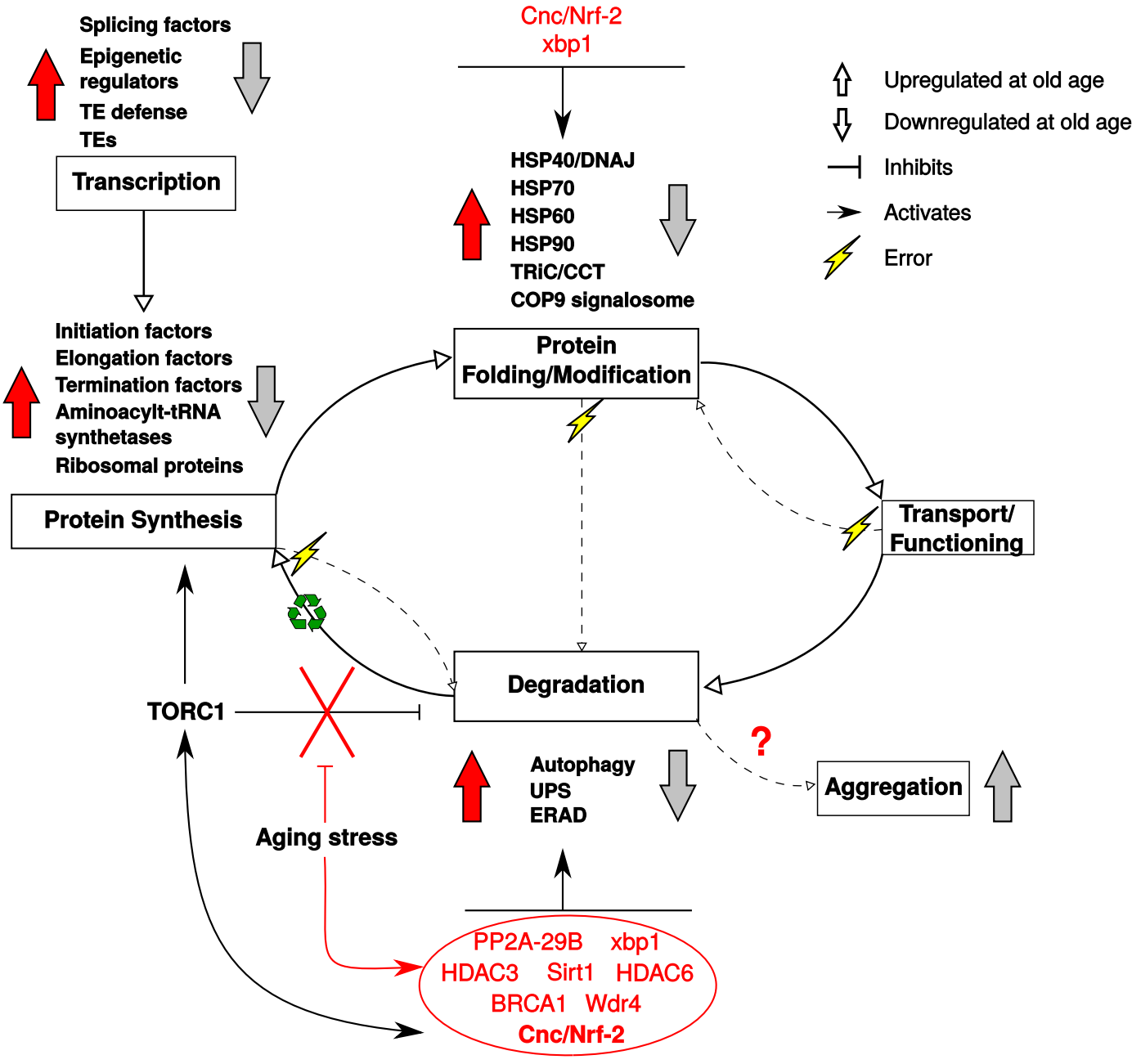
Splicing factors
Epigenetic regulators
TE defense
TEs
Transcription
Cnc/Nrf-2
xbp1
HSP40/DNAJ
HSP70
HSP60
HSP90
TRiC/CCT
COP9 signalosome
Upregulated at old age
Downregulated at old age
Inhibits
Activates
Error
Initiation factors
Elongation factors
Termination factors
Aminoacylt-tRNA synthetases
Ribosomal proteins
Protein Folding/Modification
Protein Synthesis
Transport/ Functioning
Degradation
TORC1
Aging stress
Autophagy
UPS
ERAD
?
Aggregation
PP2A-29B xbp1
HDAC3 Sirt1 HDAC6
BRCA1 Wdr4
Cnc/Nrf-2

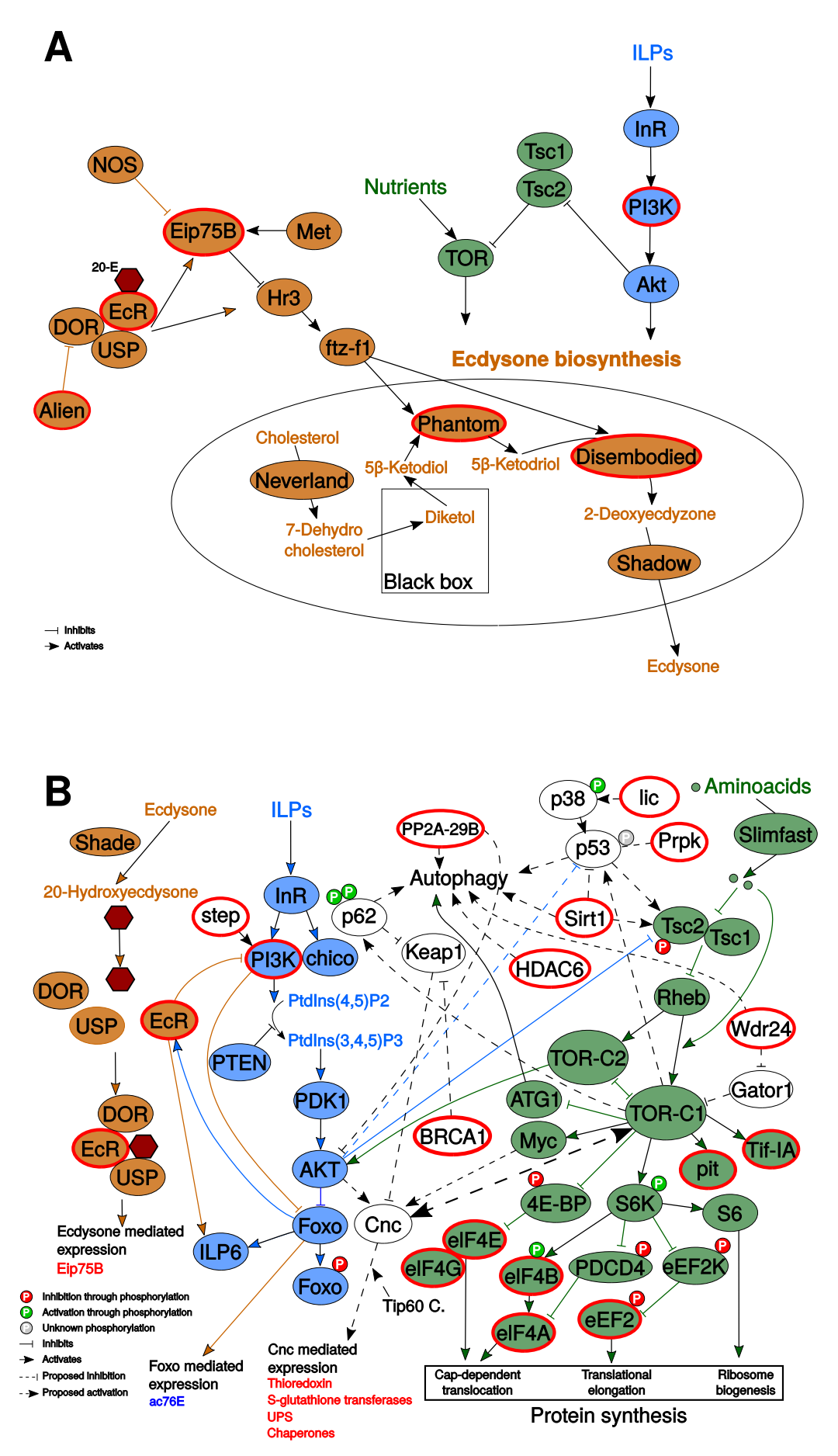
A
ILPs
InR
Tsc1
Tsc2
PI3K
Akt
Nutrients
TOR
NOS
Eip75B
Met
20-E
EcR
DOR
USP
Alien
Hr3
ftz-f1
Ecdysone biosynthesis
Phantom
Cholesterol
Neverland
5β-Ketodiol
5β-Ketodriol
Disembodied
7-Dehydro cholesterol
Diketol
Black box
2-Deoxyecdyzone
Shadow
Ecdysone
Inhibits
Activates
B
Ecdysone
Shade
20-Hydroxyecdysone
DOR
USP
EcR
DOR
EcR
USP
ILPs
InR
step
PI3K
chico
PTEN
PtdIns(4,5)P2
PtdIns(3,4,5)P3
PDK1
AKT
Foxo
Foxo
ILP6
Ecdysone mediated expression
Eip75B
p62
Autophagy
Keap1
PP2A-29B
p38
lic
p53
Prpk
Aminoacids
Slimfast
Sirt1
Tsc2
Tsc1
HDAC6
Rheb
Wdr24
TOR-C2
Gator1
ATG1
TOR-C1
BRCA1
Myc
Tif-IA
pit
4E-BP
S6K
S6
Cnc
eIF4E
eIF4G
eIF4B
PDCD4
eEF2K
eEF2
eIF4A
Tip60 C.
Cnc mediated expression
Thioredoxin
S-glutathione transferases
UPS
Chaperones
Foxo mediated expression
ac76E
Cap-dependent translocation
Translational elongation
Ribosome biogenesis
Protein synthesis
Inhibition through phosphorylation
Activation through phosphorylation
Unknown phosphorylation
Inhibits
Activates
Proposed Inhibition
Proposed activation